REPUBLIC OF TURKEY
ISTANBUL GELISIM UNIVERSITY
INSTITUTE OF GRADUATE STUDIES

Department of Electrical and Electronics Engineering

DESIGN AND IMPLEMENTATION 5G ANTENNA WITH DOUBLE NOTCH

Master Thesis

SHAYMAA ALAULDDIN ABDUWAHHAB ALEZZ

Supervisor

Asst. Prof. Dr. Ahmed Amin Ahmed SOLYMAN

Istanbul – 2022

THESIS INTRODUCTION FORM

Name and Surname	**:**	Shaymaa Alaulddin Abduwahhab ALEZZ
Language of the Thesis	**:**	English
Name of the Thesis	**:**	Design and Implementation 5G Antenna with Double Notch
Institute	**:**	Istanbul Gelisim University Institute of Graduate Studies
Department	**:**	Electrical and Electronics Engineering
Thesis Type	**:**	Master
Date of the Thesis	**:**	03/08/2022
Page Number	**:**	101
Thesis Supervisors	**:**	Asst. Prof. Dr. Ahmed Amin Ahmed SOLYMAN
Index Terms	**:**	Ultra-Wide Band (UWB) antennas, 5G application, Millimeter wave (mm-Wave), Federal Communications Commission (FCC) authorizes
Turkish Abstract	**:**	Bu tezin temel amacı, kullanılabilecek mükemmel bant genişliği ve kazancı olan iki kompakt anten oluşturmaktır.
Distribution List	**:**	1. To the Institute of Graduate Studies of Istanbul Gelisim University 2. To the National Thesis Center of YÖK (Higher Education Council)

Signature

Shaymaa Alaulddin Abduwahhab ALEZZ

REPUBLIC OF TURKEY
ISTANBUL GELISIM UNIVERSITY
INSTITUTE OF GRADUATE STUDIES

Department of Electrical and Electronics Engineering

DESIGN AND IMPLEMENTATION 5G ANTENNA WITH DOUBLE NOTCH

Master Thesis

SHAYMAA ALAULDDIN ABDUWAHHAB ALEZZ

Supervisor

Asst. Prof. Dr. Ahmed Amin Ahmed SOLYMAN

Istanbul – 2022

DECLARATION

I hereby declare that in the preparation of this thesis, scientific and ethical rules have been followed, the works of other persons have been referenced in accordance with the scientific norms if used, and there is no falsification in the used data, any part of the thesis has not been submitted to this university or any other university as another thesis.

Shaymaa Alaulddin Abduwahhab ALEZZ

…/…/2022

TO ISTANBUL GELISIM UNIVERSITY

THE DIRECTORATE OF INSTITUTE OF GRADUATE STUDIES

The thesis study of Shaymaa Alaulddin Abduwahhab ALEZZ titled as Design and Implementation 5G Antenna with Double Notch has been accepted as MASTER THESIS in the department of ELECTRICAL AND ELECTRONIC ENGINEERING by our jury.

Director *Asst. Prof. Dr. Ahmed Amin Ahmed SOLYMAN*

(Supervisor)

Member *Asst. Prof. Dr. Musaria Karim MAHMOOD*

Member *Asst. Prof. Dr. Mahmoud H.K. AL DABABSA*

APPROVAL

I approve that the signatures above signatures belong to the aforementioned faculty members.

... / ... / 20..

Prof. Dr. İzzet GÜMÜŞ

Director of the Institute

SUMMARY

Over time, the new demand for separate multiplicand antennas to be used in distant communication frameworks has gained increasing attention and interest. UltraWide Band (UWB) antennas are presented as a new solution to this problem because of their benefits, such as decreased volume, simplicity, simple fabrication process, and integration with integrated circuits (IC). The Federal Communications Commission (FCC) has designated the frequency range (3.1 to 10.6) GHz as a UWB, the unused band. UWB spectrum antennas come in various shapes: rectangular, graduated elliptical, square, triangular, circular, hexagonal, and ring. This thesis aims to create two compact antennas with excellent bandwidth and gain that can be used in most wireless applications. The proposed antennas were created, studied, and simulated using the Microwave Studio Simulation Tool (CST) from Computer Simulation Technology. A range of parametric studies has been used to explain the benefits of antennas based on various engineering factors. This thesis simulated two alternative antenna designs (elliptical and semi-rectangular) to span different spectra. Featured as an elliptical, Elliptic Patch UWB Antenna suggests this antenna consists of a square patch (16 x 12 mm 2). In order to achieve the features of the serrated triple strip, a double semicircle hole is drilled from the radiating patch and ground. The recommended antenna can work for applications that can be used in civil, military, and government organizations for weather monitoring, Etc. This antenna has a broad bandwidth from 3 to 13 GHz and 50 feed lines. The semi-rectangular Patch antenna comprises a (16×12 mm2) square patch. In order to achieve triple-notched band features, a dual semicircle slot is itched from both the radiation patch and the ground.

.

Keywords: Ultra-Wide Band (UWB) antennas, 5G application, Millimeter wave (mm-Wave), Federal Communications Commission (FCC) authorizes.

ÖZET

Zamanla, uzak iletişim çerçevelerinde kullanılacak ayrı çoklu antenlere yönelik yeni talep, artan bir ilgi ve ilgi kazanmıştır. Ultra Geniş Bant (UWB) antenler, azaltılmış hacim, basitlik, kolay üretim süreci ve entegre devreler (IC) ile entegrasyon gibi faydaları nedeniyle bu soruna yeni bir çözüm olarak sunulmaktadır. FCC, frekans aralığını (3.1 ila 10.6) GHz bir UWB olarak kullanılmayan bant olarak belirlemiştir. UWB spektrum antenleri, dikdörtgen, dereceli eliptik, kare, üçgen, dairesel, altıgen ve halka şekilleri dahil olmak üzere çeşitli şekillerde gelir. Bu tezin temel amacı, kullanılabilecek mükemmel bant genişliği ve kazancı olan iki kompakt anten oluşturmaktır. Çoğu kablosuz uygulamada. Önerilen antenler, Computer Simulation Technology'den Microwave Studio Simulation Tool (CST) kullanılarak oluşturuldu, incelendi ve simüle edildi. Çeşitli mühendislik faktörlerine dayalı olarak antenlerin faydalarını açıklamak için bir dizi parametrik çalışma kullanılmıştır. Bu tezde farklı spektrumları kapsayacak şekilde iki alternatif anten tasarımı (eliptik ve yarı dikdörtgen) simüle edilmiştir. Eliptik olarak sunulan Eliptik Yama UWB Anteni, bu antenin kare bir parçadan (16 x 12 mm 2) oluştuğunu gösterir. Tırtıklı üçlü şeridin özelliklerini elde etmek için, yayılan yama ve zeminden bir çift yarım daire delik açılır. sivil, askeri ve devlet kurumlarında hava durumu izleme vb. amaçlarla kullanılabileceği uygulamalar için çalışır. 3 ila 13 GHz bant genişliği ve 50 besleme hattı ile. Yarı Dikdörtgen Yama anteni, kare bir parçadan (16×12 mm2) oluştuğunu düşündürür. Üç çentikli bant özelliklerini elde etmek için, hem radyasyon yamasından hem de zeminden çift yarım daire bir yuva çizilir.

Anahtar Kelimeler: Ultra Geniş Bant (UWB) antenler, 5G uygulaması, Milimetre dalga (mm-Dalga), Federal İletişim Komisyonu (FCC) yetki veriyor.

TABLE OF CONTENTS

CHAPTER THREE

PROPOSED ELLIPTIC PATCH UWB ANTENNA

CHAPTER FOUR

PROPOSED SEMI-RECTANGULAR PATCH UWB ANTENNA

CHAPTER FIVE

CONCLUSION AND RECOMMENDATIONS FOR FUTURE WORK

ABBREVIATIONS

Abbreviation	Meaning
2G	Second- generation
3D	Three-Dimensions
3G	Third-generation
4G	Fourth- generation
5G	Fifth- generation
BW	Bandwidth
CST	Computer Simulation Technology
FCC	Federal Communications Commission
FR4	Flame Resistant 4
GHz	Gigahertz
GPS	Global Positioning System
GSM	Global System for Mobile Communications
HDR	High-data-rate
HLAN	Hyper Local Area Network
IEEE	Institute of Electrical and Electronics Engineers
IMT	International Mobile Telecommunications
INSAT	Indian National Satellite Systems
Kbps	Kilobits per second
LDR	Low-data-rate
Mbps	Mbps Megabits per second

LIST OF TABLES

LIST OF FIGURES

PREFACE

I would like to thank my respected professor **Asst. Prof. Dr. Ahmed Amin Ahmed Solyman** for his assistance with preparing and writing my thesis. I also like to thank the thesis jury members for their assistance in managing and moving this thesis ahead with their insightful remarks and ideas throughout the process.

Finally, I would like to thank my family for their support.

CHAPTER ONE

GENERAL INTRODUCTION

1.1 5G Communications

The term 5G (fifth-generation mobile networks or fifth-generation wireless systems) refers to the next critical phase of mobile telecommunications technologies following 4G. 5G is expected to be a mobile communications technology accessible after 2020 (Agarwal, Misra, Agarwal, & Engineering 2015). Since the first generation of mobile network standards in 1982, a new generation has emerged every ten years. These standards were developed to address the demands of today's and tomorrow's mobile customers. However, worldwide mobile traffic is increasing exponentially every year, and this trend is expected to continue in the near future (Gampala & Reddy 2016).

Global mobile data traffic will continue to expand rapidly in the future decade. Naturally, there is growing concern that the current capacity of 4G wireless networks will be insufficient in the long term. In recent years, several research foundations and commercial partners have been exploring the 5th generation (5G) mobile network, which enhances capacity, latency, and mobility (Hong, Ko, Lee, & Baek 2015). Millimeter wave (mm-wave) bands have been getting much attention as different spectrum bands for 5G cellular networks due to spectrum shortages in traditional microwave bands (Hong, Baek, Lee, & Kim 2014).

The primary aim of 5G will be to enhance network capacity while improving coverage at a lower cost. The "capacity" goal is the most critical since it directly relates to increased customer demand for faster and higher data rates. Peak data rates of 10 Gb/s for static users, 1 Gb/s for mobile users, and more than 100 Mb/s in urban areas. Massive MIMO is the approach being investigated to meet these high data rate goals (Gampala & Reddy 2016).

Massive MIMO: Extending the multi-user MIMO concept to hundreds of base station antennas dramatically improves user performance and network capacity by offering beam-shaped data transmission and interference management. Increased antenna gains are needed to compensate for the significantly increased path loss at extremely high frequencies, which may be accomplished

by increasing the number of antennas at the base station (Ahmadi 2016). 5G research and development aims for sub-1ms latency and lower battery consumption than 4G equipment (Ahmed, Haggag, & Shaker).

Moving to mm-wave frequencies for 5G mobile stations necessitates the development of new antenna design approaches for mobile-station (MS) and base station (BS) systems. The smaller antennas in an array may be joined to make an effective beam-steerable phased array antenna, which is a critical component of 5G cellular networks (Ojaroudiparchin, Shen, & Fr 2015). Because of new uses outside of personal communications, the number of devices might reach tens or hundreds of billions by the time 5G is fully implemented (Andrews et al., 2014; Liu, Sun, Sharma, Sharma, & Dhiman, 2021).

1.2 Background

Table 1.1 shows the various generations of mobile communication technologies. The mobile phone network has historically been classified into four generations, each with distinct features that set it apart from the others. Each generation differs from the others in terms of frequency, data rate, the maximum number of users, and network coverage region.

Table 1. 1 Generational Breakdown of Mobile Communications

Cellular Phone Generation	1G	2G	3G	4G	5G
1st Year Deployment	1981	1992	2001	2010	2020
Peak Supported Data Rate	2 Kbps	64 Kbps	2 Mbps	100 Mbps	10 Gbps
Frequency	900 MHz	900 MHz and 1.8 MHz	800,900 MHz and 1700 to 1900 MHz 2100 MHz	800 MHz, 900 MHz, 1800 MHz, 2100 MHz, and 2600 MHZ	28 GHz, 37 GHz, 39 GHz, and 64-71 GHz
General Functional Description	Analog Cellular Phones	Digital Cellular Phones (GSM/CDMA)	First Mobile Broadband Utilizing IP Protocols (WCDM 2000)	The Mobile Broadband on Unified Standard (LTE)	Tractile Internet Enhanced M2M Communications Network

1.3 Mm-Wave Planar Antennas

The demand for additional spectrum, as well as the need for high-speed cellular communications, has prompted the use of millimeter wave (mm-wave) carrier frequencies in future cellular networks, which utilize high-gain adaptive antennas (Jijo et al., 2021; Zhao et al., 2013).). The mm-wave spectrum has sparked much attention due to the large bandwidth available (Kim,

Bang, & Sung 2014). The millimeter-wave frequency range extends from 30 to 300 GHz, with wavelengths ranging from 10 to 1 mm. Due to the high cost and restricted availability of electronic equipment at these frequencies, mm-wave frequencies have traditionally been employed primarily for defense and radio astronomy purposes. Because of the rapid advancement of silicon technology and the rapidly expanding mm-wave application markets (such as automotive radars, high-resolution imaging, and high-definition video transfer requirements), broadband, highly integrated, low-power, and low-cost wireless systems, including high-efficiency planar antennas, are required (Alhalabi 2010). Due to their low cost, simplicity of fabrication, and promise of high-efficiency operation, integrated planar antennas have sparked much interest in mm-wave applications in recent years. The small wavelength allows for compact and efficient antennas at mm-wave frequencies. For efficient radiation, physical principles mandate that antenna size is on a half wavelength or more significant. As a result, antennas with f = 30 - 300 GHz are physically small yet electrically large enough to broadcast effectively. However, because losses at mm-wave frequencies are higher than at lower frequencies, the antenna designer must carefully construct the antenna and choose the appropriate substrate to minimize losses and achieve high radiation efficiency (Alhalabi 2010). Due to their short wavelength, the mm-wave antennas are smaller than traditional cellular frequency waves. Because of the tiny antenna size makes precise beamforming or massive MIMO technology possible (Federico, Caratelli, Theis, Smolders, & Propagation, 2021; Hong et al., 2015). The antenna should have a gain of at least 12 dB and a bandwidth of more than 1 GHz to meet 5G standards (Nor, Jamaluddin, Kamarudin, & Khalily, 2016).

1.4 Why at 28 GHz?

Due to negligible atmospheric absorption, there is an unoccupied or underused Local Multipoint Distribution Service (LMDS) broadband spectrum at 28 GHz, which has a very similar free space path loss to today's 1-2 GHz cellular bands. Furthermore, with high gain, adaptive antennas, and cell sizes on the order of 200 meters rain attenuation and oxygen loss are not dramatically enhanced at 28 GHz and offer superior propagation circumstances to today's cellular networks (Zhao et al. 2013). At 28 GHz, air absorption is minimal (0.06 dB/km), as illustrated in Figure 1.1 (MacCartney, Zhang, Nie, & Rappaport 2013).

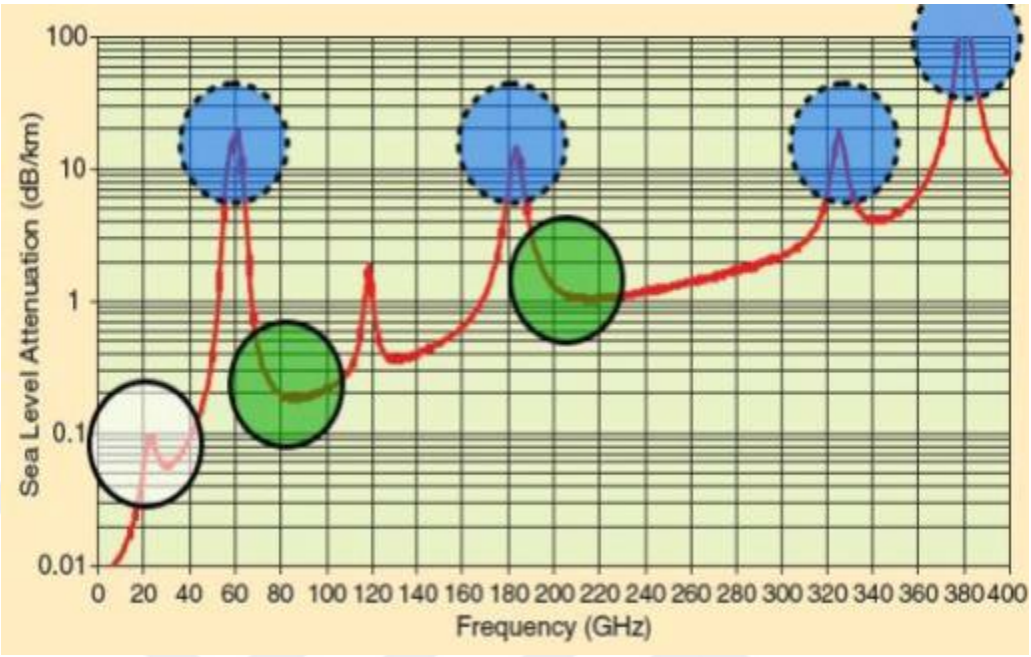

Figure 1. 1 Air Attenuation at Different Frequency Bands (MacCartney et al. 2013).

1.5 Literature review

Several mm-wave planar antennas designed for 5G communication systems have been explored and constructed:

Senić, Živković, Šimić, and Šarolić, 2014 (Senić, Živković, Šimić, & Šarolić, 2014), present a parametric investigation of the impact of the loss tangent on antenna parameters. The thesis conducts a similar parametric investigation using all substrate properties (loss tangent tan δ, dielectric constantε_r, and substrate thickness). Yu, Zhang, and letters (2003) (Yu, Zhang, & letters 2003) developed a microstrip grid array antenna on an FR4 substrate using standard PCB technology. The antenna features an S11 bandwidth of 7.16 GHz and a gain of 12.66 dB at 29.2 GHz with a -10 dB S11 bandwidth from 23.86 to 31.02 GHz. However, a lossy material, such as FR4, results in low radiation efficiency.

A 28 GHz mesh-grid antenna array is presented by Hong et al. (2014) (Hong et al. 2014). The array emits a fan-beam-like radiation pattern, with the main radiating structure consisting of a via array within a 10-layer FR4 PCB. The suggested array has a -10 dB S11 bandwidth> 3 GHz and a single element simulated gain of 3.5 dB, which is more than the 10.9 dB gain of a 16-element

array. However, adopting multilayer technology in mobile antenna design increases design and fabrication complexity, resulting in a costly device. A printed Yagi-Uda antenna constructed on a 10-layer FR4 substrate with a total thickness of 0.8 mm is used in the phased array. Alreshaid, Hammi, Sharawi, and Sarabandi (2015) proposed a 28 GHz slot antenna array with 5% bandwidth and a gain of 13dB (Alreshaid, Hammi, Sharawi, & Sarabandi 2015b). The provided eight-element arrays have an occupied size of just 29.928.70.13 mm3. Alreshaid, Hammi, Sharawi, and Sarabandi (2015 a) proposed a switched beam planar array with a central frequency of 28.5 GHz and a bandwidth of 1 GHz. (Alreshaid, Hammi, Sharawi, & Sarabandi 2015a). The suggested antenna has an 8 – 12 dB gain. The beams emitted by the antenna array were directed to four separate sites; ±20˚ and ± 45˚; the scanning angle must be greater than 45 for mobile antennas to perform correctly. A conformal tapered slot antenna array was presented by Ashraf, Haraz, & Alshebeili (2015) (Ashraf, Haraz, & Alshebeili 2015) with a -10 dB S11 bandwidth of 14.8 GHz. Dielectric lenses were utilized to boost antenna gain by more than 20 dB throughout a wide frequency range (24 – 40 GHz). The system employs four orthogonal independent beams that are ±14 degree angle along the co-ordinate axis. Gampala and Reddy (2016) have developed Millimeter Wave Antenna Arrays for 5G Cellular Applications (Gampala & Reddy 2016) to highlight the concept of massive MIMO, which employs antenna arrays and beamforming techniques to fulfill high data rate needs. The antenna is set to operate at 28 GHz. Ashraf et al. (2015) present a unique dense dielectric (DD) patch array antenna prototype working at 28 GHz for future fifth-generation wireless communications (5G) (Ashraf et al. 2015). In the recommended configuration, four circular-shaped DD patch radiator antenna components are supplied by a 1-to-4 Wilkinson power divider. The measured impedance bandwidth of the proposed array antenna ranges from 27 to 32 GHz for a reflection coefficient (S11) of less than 10 dB and a total realized gain of more than 16 dB. The design is based on a multilayer technology, which makes manufacturing difficult and costly. On the other hand, dual-band antennas only have a few active bands. As a result, triple and multiband antennas may be used for a more significant number of bands. Several triple band patch antennas have been reported by (Abbas et al. 2011; Basavarajappa & Vinoy, 2010; Jing et al., 2006; Kurup, Vijesh, Mohanan, Nampoori, & Bindu, 2014; Nella & Gandhi, 2017; Nikmehr & Moradi, 2010; Pokorný, Horák, & Raida, 2008; Vinci & Weigel, 2010; Wadekar & Khobragade, 2015) for the intended applications.

1.6 Thesis motivation

This research has required a thorough examination of several aspects that affect antenna performance (such as antenna type, feeding mechanism, substrate dielectric constant, substrate thickness, substrate loss tangent, Etc). The outcomes of this study can be used as a design reference for 5G mm-wave antenna builders. The study's value is demonstrated by developing a planar antenna suited for 5G communication networks. The suggested antenna operates in the 28 GHz frequency band and has the following design characteristics. The recommended antenna has a wide bandwidth of more than 1 GHz, with an excellent 50 Ω impedance matching with S11 < -10 dB and consistent radiation patterns capable of supporting the projected high data rates of future 5G networks. The suggested antenna has high radiation efficiency to compensate for the additional path loss at mm-wave frequencies. Higher antenna efficiency reduces the need for power amplifiers and extends the life of mobile phone batteries. Because the mobile phone orientation does not remain constant during typical operation, it features multi-polarization capacity to decrease polarization mismatch losses. The suggested antenna design was refined into a multi-element array configuration for higher gain and a better signal-to-noise ratio (SNR).

CHAPTER TWO

UWB ANTENNA

1.1 UWB Antenna

Global System of Mobile, Wi-Fi, and Wi-MAX applications are prevalent in today's wireless communication because they allow SMS, audio and video discussions, high-speed data transmission, and internet access anytime and anywhere. Mobile phones, laptops, and other portable devices are frequently linked to these apps. These devices incorporate a variety of antennas in order to deliver the necessary wireless applications. Despite these restrictions, microstrip antennas are frequently employed in today's wireless communication systems.

Descamps developed the term "microstrip antenna" (MSA) in 1953. However, Munson and Howell's work in the 1970s resulted in constructing these antennas. Since then, there has been a remarkable advancement in research in microstrip antennas.

Table 2. 1 A list of the frequency bands designated for use by various types of mobile wireless communication systems

(Bankey & Kumar 2016; Nella & Gandhi 2017).

Wireless Use	Frequency Band (MHz)
Global System of Mobile 850 (AMPS)	824-894
Global System of Mobile 900	890-960
Global Position System	1565-1585
Global System of Mobile 1800 (DCS 1800)	1710-1885
Global System of Mobile 1900 (PCS 1900, CDMA 1900)	1850-1990

Universal Mobile Telecommunications Service (W-CDMA, IMT 2000)	1885-2200
Long-Term Evolution 2300 (Band-40)	2300-2400
Wi-Fi/WLAN (ISM 2450) (IEEE 802.11 b/g/n)	2400-2495
Extended Universal Mobile Telecommunications Service (LTE 2600 Wi-MAX 2500)	2500-2690
Worldwide Interoperability for Microwave Access 3500	3300-3600
Wi-Fi/WLAN (IEEE 802.11 y)	3650-3700
Wi-Fi/WLAN (HIPERLAN, U-NII) (IEEE 802.11 a/h/j)	5150-5825

1.2 Straight Microstrip Antennas

Microstrip antennas for single, dual, triple, and multiband portable wireless applications are covered in this area. Many single-band microstrip antennas are discussed at the beginning of the study. These antennas need a sizeable operating spectrum to be helpful in a wide range of situations. Nevertheless, as previously indicated, the bandwidth of typical patch antennas is reduced. However, according to the literature (Fares & Adachi, 2010; Nella & Gandhi 2017; Patil & Rohokale 2015; Rahman et al. 2015; Rathor, Saini & Applications 2014; Saleem, Nawaz, Shabbir, Abbas & Ali 2013; Wang et al. 2012), a few approaches for increasing impedance bandwidth are discussed. We investigated many single-band microstrip antennas published in (Hsiao 2004; Nella & Gandhi 2017; Patil & Rohokale 2015; Rahman et al. 2015; Rathor et al. 2014; Saleem et al. 2013; Wang et al. 2012). There is a description of a half-U-slot modified tiny wideband patch antenna (Wang et al. 2012). The slot is added to the active patch to increase impedance bandwidth while decreasing patch size. As shown in Fig. 2.1, with a gain of 2dBi at 2.6 GHz, the proposed antenna covers the frequency range of 1.675 GHz to 2.6GHz. Low-power wireless applications such as DCS 1800, PCS 1900, Universal Mobile Telecommunications Service, Long-Term Evolution, A wireless LAN, and Worldwide Interoperability for Microwave Access are well-suited to the operational spectrum. The authors also provided the antenna's performance for various ground plane lengths in the publication.

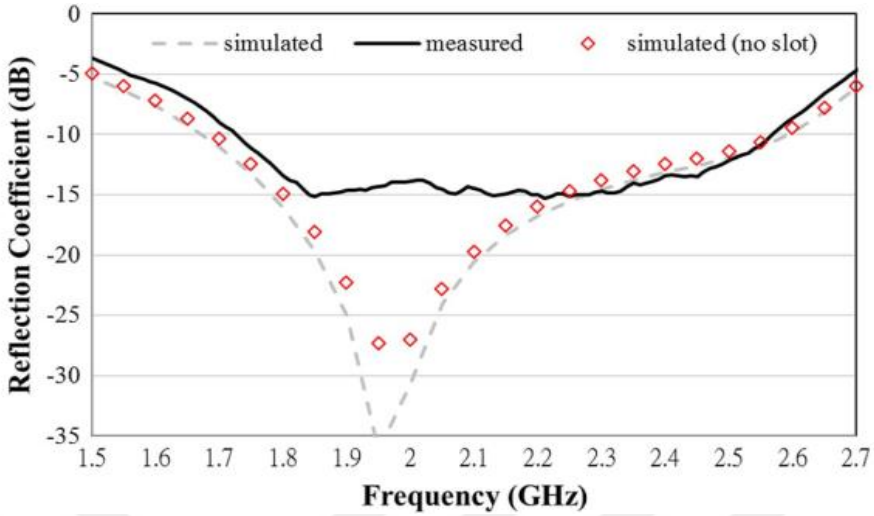

Figure 2. 1 Antenna reflection coefficients (Wang et al. 2012).

Rahman et al. (2015) addressed planar monopole antennas for GSM 1800 and 1900, Global Position System, Worldwide Interoperability for Microwave Access, Universal Mobile Telecommunications Service, and Long-Term Evolution applications. From 1.33GHz to 4.76GHz, the impedance bandwidth of this antenna is covered by –6dB. At 2.7GHz, it has a maximum gain of 3.85dBi and a maximum directivity of 5.04dBi. A dielectric substrate of 35.5mm × 75.5mm × 0.87mm is used to build the antenna. The impedance bandwidth of this antenna is improved by the capacitive effect of two parasitic elements near the feeding line and the series impedance matching effect of a loop monopole capacitor.

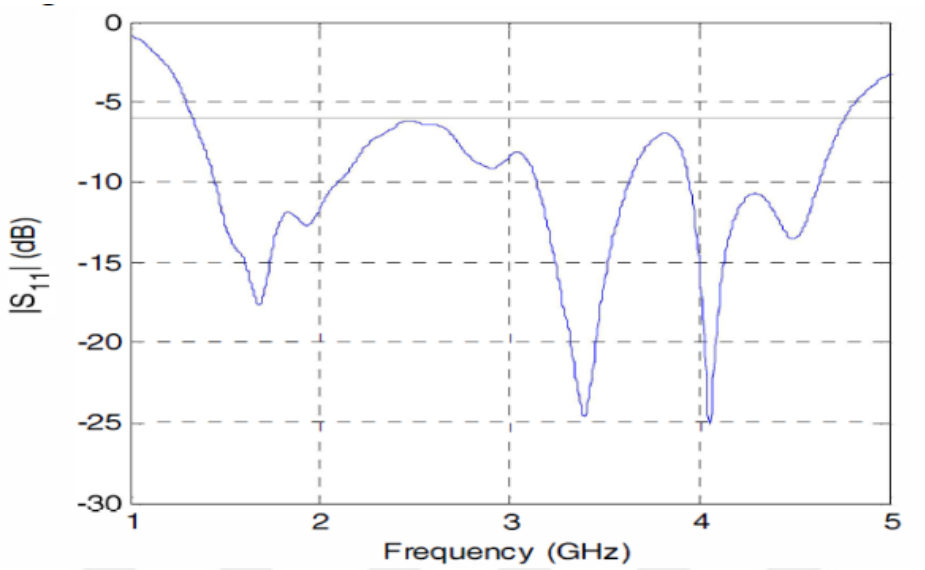

Figure 2. 2 an extensive range of frequencies

An extensive range of frequencies can be covered by ultra-wideband antennas, which can be used in various ways. Some frequencies are unnecessary for portable system applications in the antenna's frequency range (Saleem et al., 2013). As a result, these antennas may experience interference. These concerns may be alleviated by using double, triple, and multiband antennas, which can cover a wide range of wireless applications.

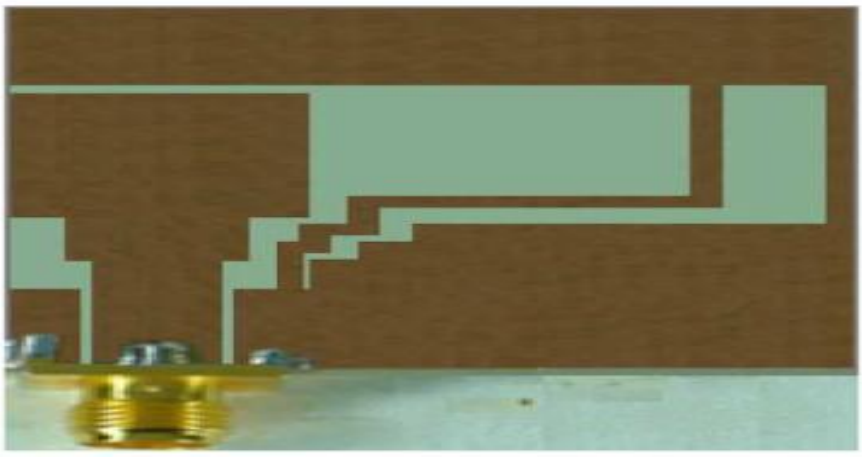

Figure 2. 3 Fabricated antenna prototype (Naser-Moghadasi, Sadeghzadeh, Asadpor, Virdee, & letters 2013).

Several twins, triple, and multiband microstrip antennas are described in (Hsu & Wu, 2013; Jayasinghe et al. 2012; Kuo, Huang, & Jan 2006; Naser-Moghadasi et al. 2013; Su, Chien, Tang & Wong, 2005; Zhang, Li, & Tentzeris 2011). Various dual band antennas are being researched by (Hsu & Wu 2013; Jayasinghe et al., 2012; Kuo et al., 2006; Naser-Moghadasi et al., 2013; Su et al. 2005; Zhang et al., 2011) for altered wireless tenders. Naser-Moghadasi et al. (2013) have developed coplanar waveguide fed antennas for the Global System of Mobile 1800, 1900, and a wireless LAN. Two conducting plates are connected via a high impedance step-shaped microstrip line to create the ground plane. Adding a 5.3GHz mode to the initial antenna response is done by this strip line. This antenna has two planned frequency bands of operation, 1.6 GHz to 1.85 GHz and 4.94GHz to 5.8GHz, and it is printed on a small dielectric substrate measuring in the dimension 20mm×17mm×1mm. In the Global System of the Mobile band, circular PolarizationPolarization is the antenna's most crucial feature.

Fayasinghe et al. (2012). discuss a multiband planar monopole antenna for ultra-thin mobile devices. The FR-4 substrate is 50mm × 110mm × 0.8mm thick and is used to print this antenna. It has a bandwidth cut-off of 6 dB and operates at frequencies between 0.885 GHz and 0.962 GHz and 1.69 GHz and 3.8 GHz. The two resonating branches of this antenna, the C-shaped branch and the meandering line branch linked with an L-strip, are the two resonating branches, as shown in Figure 2.4. The meandering line branch with an L-strip gets the lower frequency band, while the C-shaped branch gets the higher frequency band.

At the lower frequency band border, C-shaped branch length is computed as 1/4, whereas meandering line branch length is approximated as 3/8. Free space and a mobile environment comprising a portable plastic enclosure, a giant metallic display screen, and a battery are used to test the proposed antenna's performance.

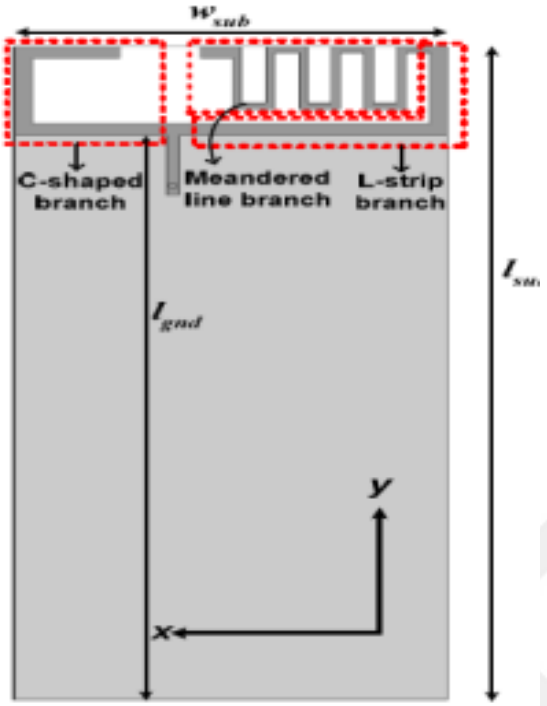

Figure 2. 4 Structure of the proposed antenna

(Bharti, Pandey, Singh, & Meshram 2015)

Jayasinghe et al. (2012) reported that an algorithm optimization technique was used in the microstrip antenna design. This antenna has a frequency range of 880MHz to 960MHz and from 1700MHz to 2520MHz for Global System of Mobile, Universal Mobile Telecommunications Service, and Long-Term Evolution, as well as Bluetooth applications. Their initial design was a rectangular patch antenna that could operate between 2090MHz and 2300MHz. An algorithm optimization process was then employed to change the antenna recommendation. As seen in Fig. 2.5, this technique allows the patch to be separated into a limited number of closely spaced cells. A shorting pin is also added in the suggested design for better impedance matching.

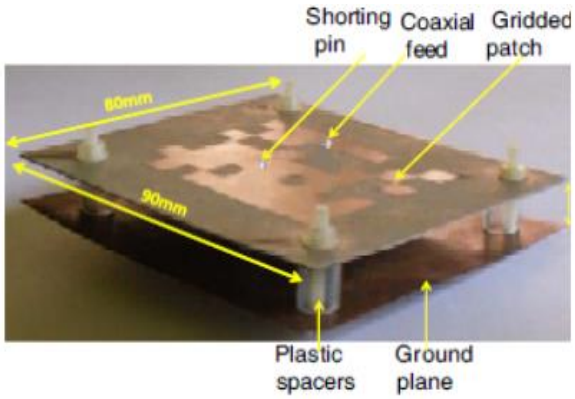

Figure 2. 5 The microstrip antenna's design(Jayasinghe, Anguera, & Uduwawala 2012).

An antenna for GSM and Wi-Fi with a microstrip line feed is shown in this paper (Hsu & Wu, 2013). A 64mm × 48mm × 1.6mm dielectric substrate is used to print the antenna. Two different frequencies can be tuned simultaneously by using this antenna's rectangular slotted modified ground plane and microstrip line (Fig.2.6). It has maximum gains of 4.86dBi and 4.63dBi at 1.8GHz and 5.8GHz, respectively. When a rectangular slot is lengthened or widened, its return loss performance is indicated in the paper.

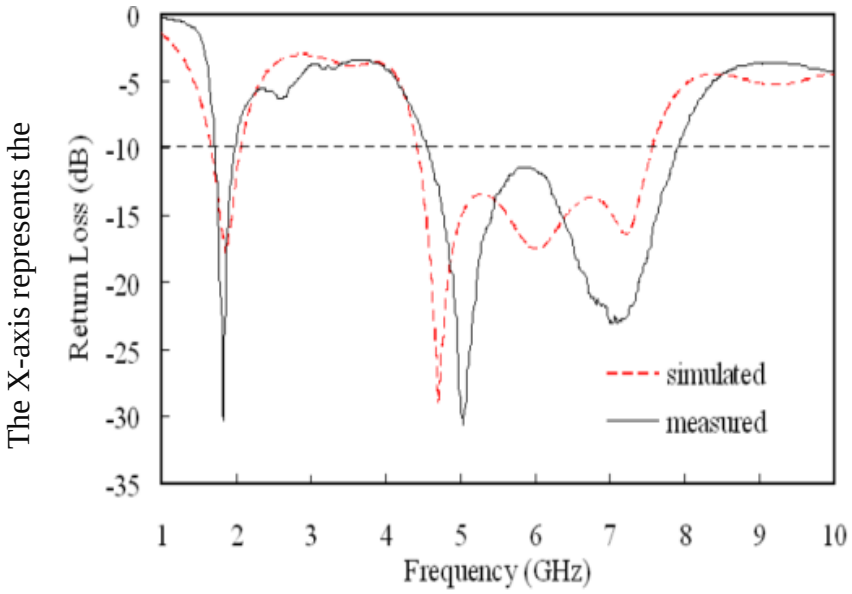

the y-axis represents the return loss in dB

Figure 2. 6 Loss-return pattern(Hsu & Wu, 2013).

On the other hand, dual-band antennas have a restricted number of operational bands. Therefore, triple and multiband antennas may be chosen for a more significant number of bands. We have looked at many triple band patch antennas that were mentioned in (Abbas et al., 2011; Basavarajappa & Vinoy, 2010; Jing et al., 2006; Kurup et al. 2014; Nella & Gandhi, 2017; Nikmehr & Moradi, 2010; Pokorný et al. 2008; Vinci & Weigel, 2010; Wadekar & Khobragade, 2015) for the future applications.

In (Basavarajappa & Vinoy, 2010), The authors discussed the GSM 1800, 1900, Wireless LAN 2.4GHz, and Worldwide Interoperability for Microwave and described a microstrip antenna design with two U-slots for access purposes. This antenna can function in three frequency bands: 1.7GHz to 2.2GHz, 2.4GHz to 2.5GHz, and 5.15GHz to 5.85GHz. In their work, the scientists first devised a microstrip antenna that resonates at 2.1GHz. Two U-slots are added to the active patch to obtain two extra resonances at 1.7GHz and 5.4GHz. The lengths of the two U-slots are identical to the wavelengths at their respective resonance frequencies. As illustrated in Fig. 2.7, the suggested antenna is printed on a dielectric substrate with dimensions of 52mm×71mm (L×W).

For mobile device applications, a small triple band planar antenna is suggested (Jing et al. 2006). As seen in Fig.2.8, this antenna has three

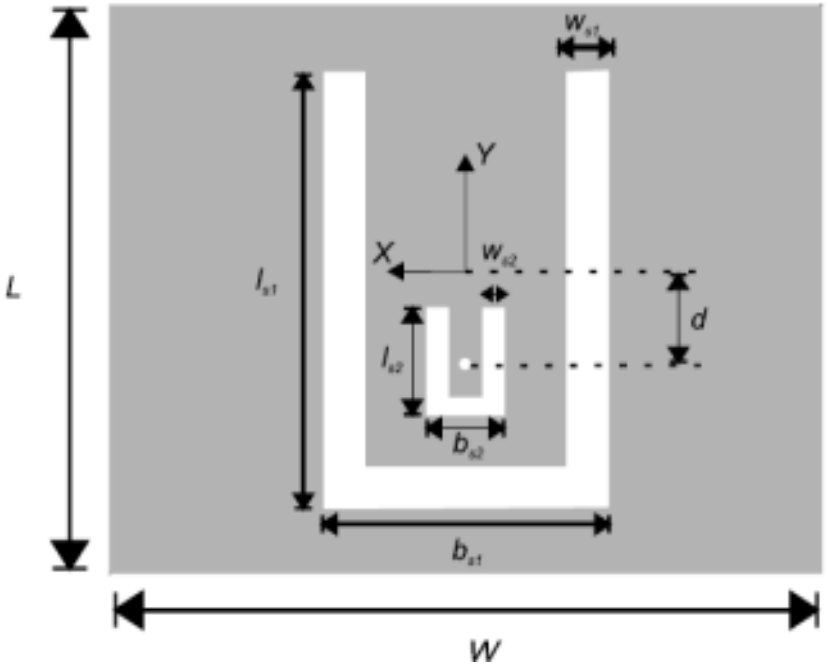

Figure 2. 2 The microstrip antenna's geometry (Basavarajappa & Vinoy 2010).

resonating branches and one tuning branch. Impedance matching is mainly accomplished with a tapered member at the feeding point. The suggested antenna has a low cost, a small footprint, and a decent radiation pattern.

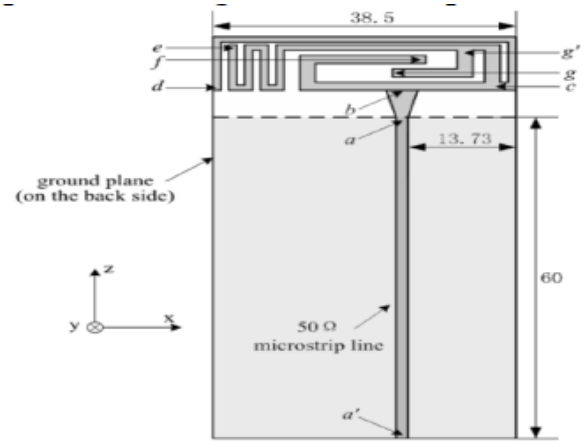

Figure 2. 3 The multiband planar antenna's topology (Jing, Du, Gong, & Letters 2006)

As shown in Fig.2.9, the antenna can span three resonating bands between 891MHz and 961MHz, 1705MHz and 2180MHz, and 2341MHz and 2941MHz. The three bands are utilized by the Global System of Mobile (900, DCS 1800, and PCS 1900), Universal Mobile Telecommunications Service, Long-Term Evolution, and Wireless LAN, among others.

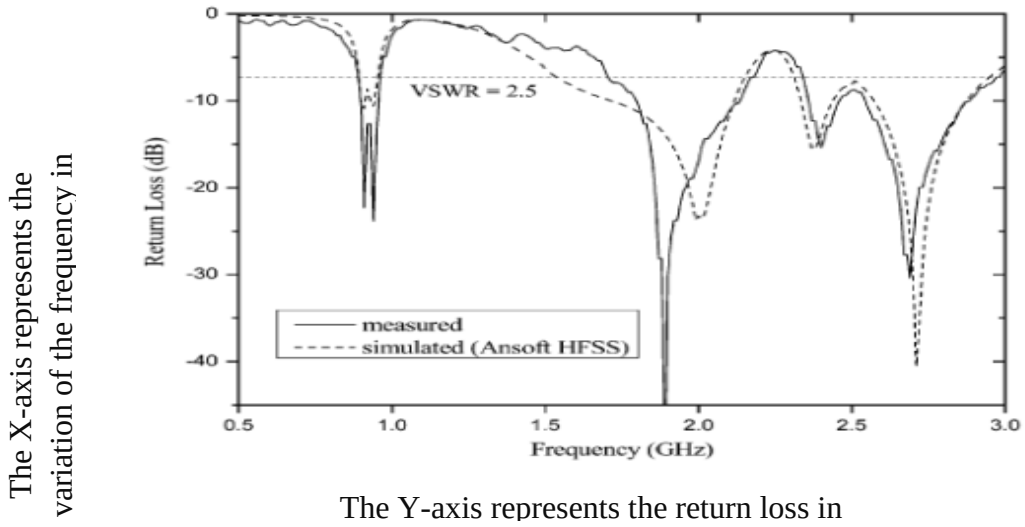

Figure 2. 4. The planar antenna's return loss performance (Jing et al. 2006)

Sharma & Hashmi (2014) introduced a tri-band slotted patch antenna for various mobile wireless applications. The active patch is 37.02 mm × 27.26 mm and is printed on a dielectric substrate of 80 mm × 78.93 mm × 1.7 mm in size. The active patch is shorted to the ground plane using a quarter-wave line and asymmetrical U-shaped microstrip slots to achieve the tri-band resonant frequency. As shown in Figure 2.10, the antenna can function in several different frequency bands, including GSM 1.8GHz, Wireless LAN 2.4 GHz, and Worldwide Interoperability for Microwave Access 3.53GHz. Simulation and actual variations in slot reflection coefficient graphs (Sharma & Hashmi 2014).

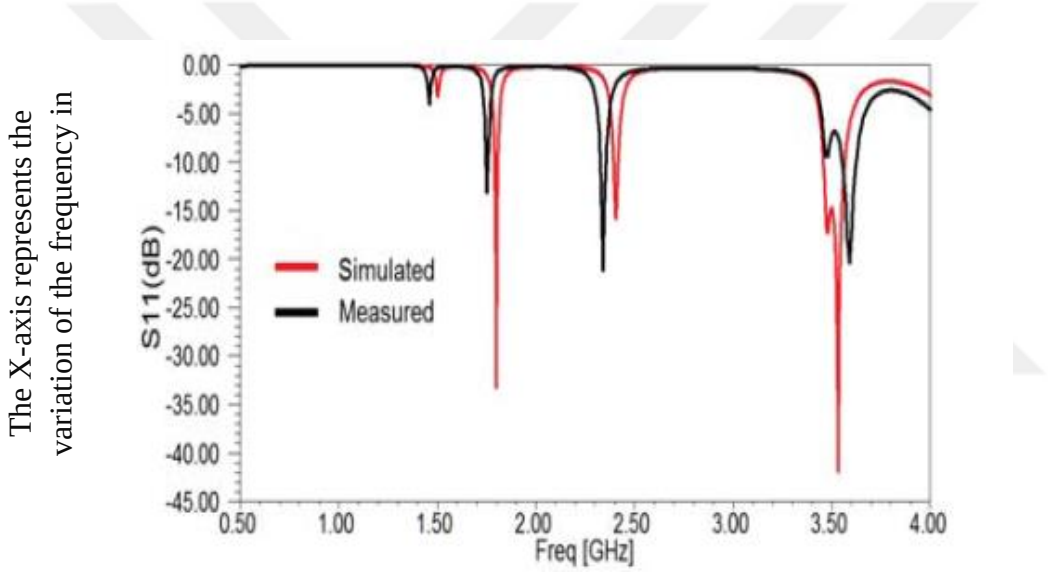

Figure 2. 5 Reflection coefficient graphs, both simulated and measured (Sharma & Hashmi 2014).

Sabri & Atlasbaf (2008) explored antennas for PCS 1900, Wireless LAN 2.4GHz, and 5GHz band applications and studied two tiny triple band microstrip annular ring slot antennas. Photonic Bandgap (PBG) structures placed on the second antenna's top layer improve the radiation performance of the first antenna. Structures like this also help reduce antenna size. Three circular ring slots are depicted in Fig. 2.11 as the ground planes for the proposed antennas. The outside

rings generate the first resonant mode, while the intermediate rings generate the second. The inner rings produce a large upper-working band by merging the third and fourth resonant modes.

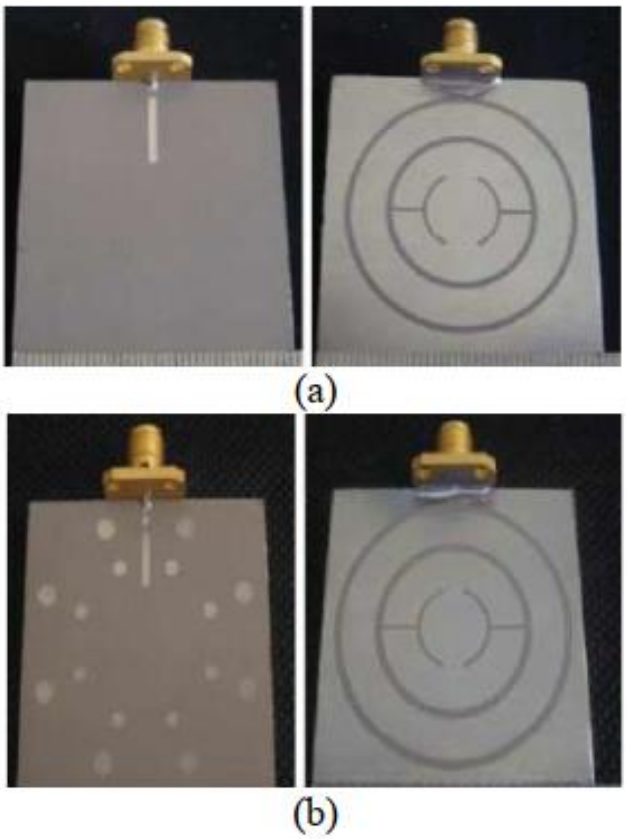

Figure 2. 6 (a) the first structure of annular ring slot antennas, and (b) the second structure of annular ring slot antennas (Sabri & Atlasbaf 2008)

2.3 Ultra-Wideband Technique

Ultra-wideband (UWB) wireless is a communication technology that uses short-pulse, low-powered radio transmissions to carry vast volumes of digital data over a wide frequency range. UWB is typically used to describe a sign or system with a substantial relative bandwidth exceeding a total bandwidth of 500 MHz. The Federal Communications Commission (FCC) authorized the unlicensed use of UWB in the frequency range of 3.1–10.6 GHz in a report and order issued in February 2002. Wireless Personal Area Network (PAN) is specified as connection, longer-range, and low-rate applications such as radar and imaging systems. There is interest in UWB technology due to its essential qualities, such as high data rate wireless technology for

many applications. However, a big issue here is the interference of bands in the (3.1-10.6) GHz region. This chapter provides an overview of UWB technology, beginning with the fundamental notions of UWB technology at a specific range of UWB, including its technique, benefits, and applications. There are various challenges in designing antennas for ultra-wideband applications. One of these challenges is miniaturizing antennas with a wide impedance bandwidth and good radiation efficiency. By substituting three-dimensional radiators with planar equivalents, a planar design may often be employed to minimize the volume of a UWB antenna. However, there is a problem with interference between the bands. The detected interference is caused by narrowband applications that are 20 dB greater than the UWB emission limit, such as wireless local area network (WLAN), global interoperability for microwave access (WiMAX), and Industrial–Scientific–Medical (ISM). At present power levels, operating UWB in the face of significant narrowband interference sources is difficult. Since the waveband was authorized and allocated a frequency range of (3.1 -10.6) GHz, (UWB) technology has emerged as one of the most promising technologies for future high-speed wireless communications, high-resolution radar, and imaging systems. The UWB antenna has piqued the interest of academics as a crucial component of the UWB system. It has appealing characteristics such as compact size, low cost, and a superb omnidirectional radiation pattern. However, there is a potential electromagnetic interference problem because there are some narrow bands for other communication systems on the broadband assigned to the UWB system, such as WiMAX operating at 3.3-3.7 GHz, WLAN operating at 5.15-5.825 GHz, and downlink - communication systems satellites with a bandwidth of 7.25-7.75 GHz. These frequencies are frequently rejected by three bandwidth stop filters coupled to a UWB antenna. However, this increases the system's complexity; the simplest solution is constructing a UWB antenna with grooved properties. UWB antennas with band grooving functions have been described, mainly with a single band for WLAN at 5.15–5.825 GHz. Several cog-banded antennas have recently been introduced. One of the significant aspects influencing the advancement of UWB technology is the design of UWB antennas. As a result, UWB antenna design has received much attention in recent years. UWB antennas must be both electrically compact and inexpensive. An omnidirectional radiation diagram must have flatness and phase linearity, as well as a constant group delay, for a UWB antenna to avoid distorting the waveform of an ultra-narrow on the order of nanoseconds electromagnetic energy pulse.

2.4 UWB Principles

Impulse radio communication systems and impulse radars both transmit brief pulses, resulting in an ultra-wideband spectrum. This communication method is classified as a pulse modulation strategy for radio applications since the data modulation is introduced using Pulse Position Modulation (PPM). The UWB transmission is noisy, making interception and detection challenges. UWB transmissions produce very minimal interference with current narrowband radio systems due to their low power spectral density. This should allow radio systems to operate without a license, depending on the attitude of national and international regulatory agencies. A carrier-free baseband broadcast is a Time-Modulated (TM) impulsive radio transmission. Impulse radio and impulse radar transmissions are distinguished from narrowband applications as well as Direct Sequence (DS), Spread Spectrum (SS), and Multi-Carrier (MC) transmissions, which may also be regarded as an (ultra) wideband approach by the lack of a carrier frequency (Oppermann, Hämäläinen, & Iinatti 2004).

2.4.1 Interference

The UWB must overlap with different structures in its wide bandwidth of operation. For instance, inside the United States, the UWB frequency variety for verbal exchange packages is 3.1 to 10.6 GHz, so it is far running with equal frequencies, consisting of cordless telephones, virtual TV (WLANs), WiMAX, and satellite TV for pc receivers, in addition to industrial and governmental structures, consisting of navigational and meteorological radar. It could overlap with a few rising structures in different countries, consisting of third-generation (3G) or fourth-generation (4G) Wi-Fi offerings. The Wi-Fi industry, governments, and regulatory bodies have accumulated a depth of studies into how UWB will interfere with different structures running inside the equal frequency bands. They all agree that any UWB transmission must be confined to avoid interference in the frequency bands. Because there is no well-known international coverage for the allocation of bandwidth, each that allocates spectrum may have a premium listing of potential receivers. For instance, in Europe, WiMAX offerings will use the 3 GHz band. As a result, any interference-mitigation strategies must be tuned (Aiello & Batra, 2006).

2.4.2 Band-Notched UWB Antenna

UWB antennas have a wide range of narrowband wireless communication, and they may cause interference with the UWB system or vice versa. Examples include IEEE 802.11a WLAN systems operating at 5.15–5.825 GHz, satellite services operating in the (4.5–5) GHz range, and IEEE 802.16 WiMAX systems operating at (3.3–3.7) GHz. The conventional way of preventing such unwanted potential interference to the UWB system is to install narrowband band-stop filters within the antenna or feed line, which increases the device's complexity and expense. The design of UWB antennas was investigated with filtering characteristics or notch-band functions by altering the current distribution direction and exploring possibilities for compact implementations. One of the easiest, most successful, and least expensive ways to achieve the goal of a band rejecting notch is to insert many slots, either on the diverging patch or on the bottom plane (Li, Li, Ye, & Mittra 2014).

2.4.3 Main Reason to Use UWB

Antenna design for (UWB) applications has several challenges, one of which is miniaturizing antennas with broad electrical phenomenon information detection and high radiation efficiency. Flat antennas are frequently used to minimize the size of UWB antennas by substituting three-dimensional radiators with flat ones, or they are simply implanted inside wireless devices or integrated with other RF circuits. In the style of a traditional UWB antenna, the radiator and ground plane shapes and the feeding structure will be optimized (Chen, See, Qing, & propagation 2007).

2.4.4 Characteristics of UWB

UWB applications have the following characteristics:

1- a minimal potential for complexity and expense.

2- a signal spectrum that looks like noise.

3- resistance to multipathing and jamming.

4- a high time-domain resolution allows for locating and tracking applications. They also have low complexity and a cheap cost (Politano et al. 2006).

The minimal complexity and low cost of UWB systems originate from the signal transmission's baseband nature. Besides, the UWB transmitter generates a brief time-domain pulse that can propagate without requiring an extra RF (Radio Frequency) mixing step. The RF mixing stage injects a carrier frequency into a baseband signal or converts the signal to a frequency with appropriate propagation characteristics. Because of UWB signals' wideband nature, it often spans frequencies employed as carrier frequencies. Without extra up-conversion, the signal will spread well. The UWB receiver also does not require the reverse procedure of down-conversion (Politano et al. 2006).

2.4.5 Advantage of UWB Applications

The UWB transmitter generates a small-time domain pulse that can spread without requiring a separate radio frequency mixing step. The RF mixing stage takes a baseband signal and 'injects' or transforms it into a frequency with favorable propagation characteristics. The comprehensive nature of the UWB signal allows it to cover commonly used carrier frequencies. Without any further up-conversion or amplification, the signal will travel well. The UWB receiver does not require the reverse down conversion process, which eliminates the need for a local oscillator, the associated expensive delay, and phase tracking loops (Tuovinen, Kumpuniemi, Yazdandoost, Hämäläinen, & Iinatti 2013). UWB can be applied in many fields, including: -

- Local & personal area network
- Wireless streaming video distribution
- Home networking
- Wireless sensor networks
- Health & habitat monitoring.

2.5 Microstrip Antenna

A square measure of various substrates can be applied to plan microstrip antennas, and their dielectric constants are usually in the range of ($2.2 \leq \varepsilon r \leq 12$) for good antenna performance. That measure is the most fascinating. Because microwave electronic equipment requires tightly regulated fields to minimize undesired radiation and coupling, thin substrates with more significant material constants help reduce component sizes. However, their higher losses make them less cost-effective and have narrower bandwidths. Because microstrip antennas are frequently integrated with various microwave electronic equipment, a compromise between good antenna performance and gate style should be found. Usually, patch antennas are also known as microstrip antennas. The solid substrate's diverging sections and feed lines are typically icon carven. Diverging patches can be rectangular, slim strip (dipole), circular, elliptical, triangular, or any other shape. Figure (2.1) depicts these and other related items. The most frequent shapes are square, rectangular, and circular because of their ease of analysis and production and appealing properties, particularly low cross-polarization radiation. Microstrip dipoles appeal because they have an enlarged information measure by definition (C. Balanis 1997).

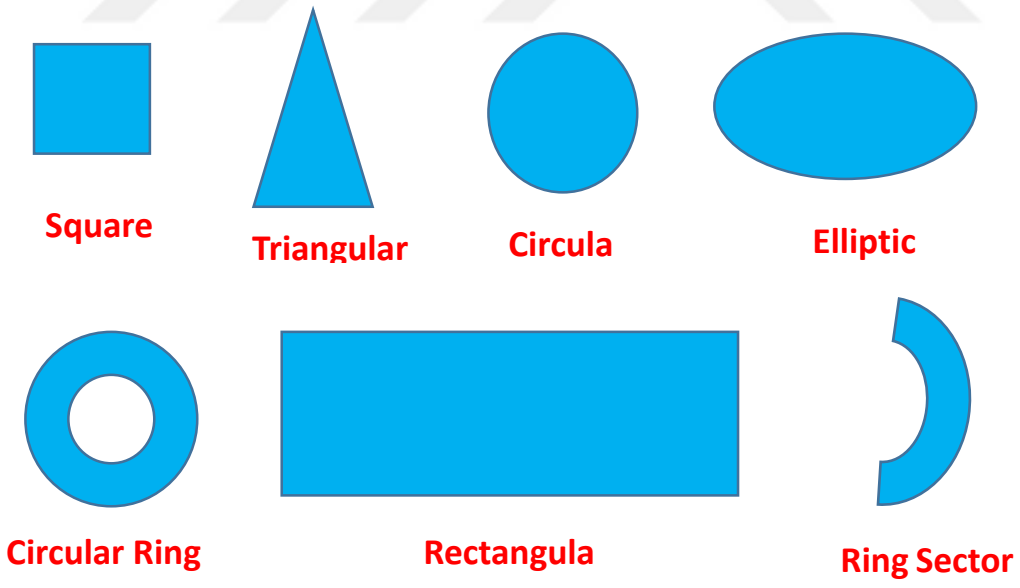

Figure 2. 7 Different structures of the Radiating Patch (C. Balanis 1997)

2.5.1 Why Microstrip Antenna

The cost of manufacturing phased array antennas rises as the number of radiating elements grows. There will be a need for phase shifters, various feeds, and multiple wires. A phased array will also take longer to build and assemble than other antenna layouts. Depending on the type of material utilized, aperture antennas can be costly. Depending on the material utilized, a horn antenna has more intricate dimensions and may be challenging to fabricate. Aperture antennas are commonly made from sheet metal to keep the structure sturdy. Different antenna components can be manufactured separately and formed together to make a single structure, although this will lengthen the manufacturing process and raise the cost. The material needed for a helix antenna is minimal. Conductive wire and a metal plate serving as a ground plane are required. The helical structure's supports could be built of wood and utilized to support the helical structure. Hand installation is required for the support mechanism. Microstrip antennas can be produced inexpensively using cheaper substrate materials, conductive materials for radioactive elements, and ground planes. Laser cutters can be used to cut out design shapes, which can be rapid (Fung 2011).

2.5.2 The Rectangular Patch Antenna

By far, the most common patch configuration is the rectangular one. It is pretty simple to evaluate it using both transmission line and cavity models, which are more accurate for thinner substrates, as seen in figure (2.12) (C. Balanis 1997).

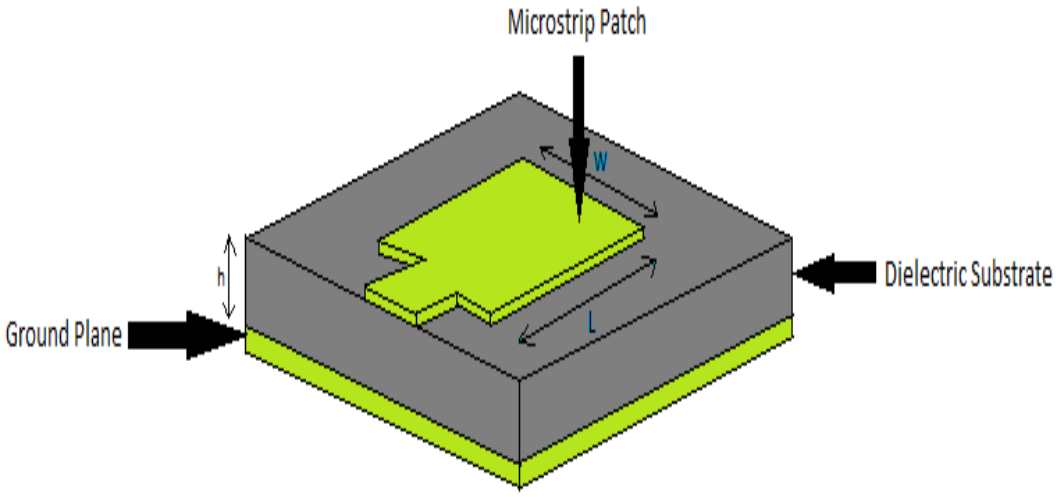

Figure 2. 8 The geometry of the rectangular microstrip patch antenna

(C. Balanis 1997).

2.5.3 The Circular Patch Antenna

Besides the rectangular patch, the most popular configuration is the circular patch or disk. The antenna will be discovered by treating the patch as a ground plane. Like the rectangular patch, the modes are supported primarily by a circular microstrip antenna whose substrate height is a little patch. This is due to the patch's dimensions and area (length and width) in the rectangular microstrip antenna. Consequently, the relative proportions of the patch's breadth and length will dynamically vary the order of the modes (width-to-length ratio). However, the circular patch has only one degree of freedom to manipulate (radius of the patch). However, there is only one degree of freedom to handle the circular patch (radius of the patch). As seen in figure (2.13), this does not change the sequence of the modes, but it does change the value of the resonant frequency (C. A. Balanis 2012).

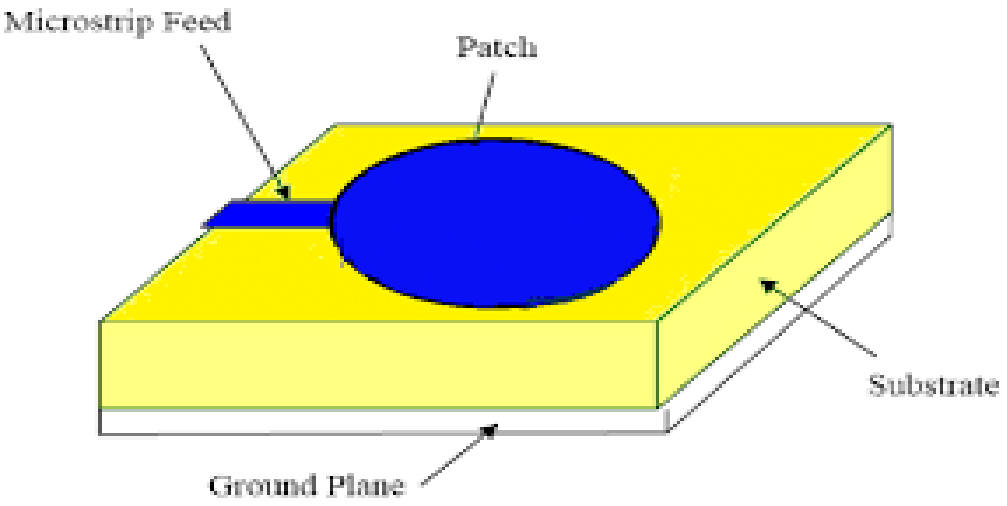

Figure 2. 9 The geometry of the circular patch antenna (C. A. Balanis 2012)

2.6 Feeding Techniques

The most common nutrition schemes are central sensor feed, microstrip line, aperture coupling, and proximity coupling. The inner conductor of a coaxial probe is connected to the antenna's radiating patch, while the outer conductor is attached to the bottom plane in coaxial probe feeding. The benefits of coaxial feeding include ease of manufacturing, ease of matching, and low radiation, while the negatives include limited information measurement and difficulty modeling, particularly for thick substrates, as seen in figure (2.14) (Singh & Tripathi 2011).

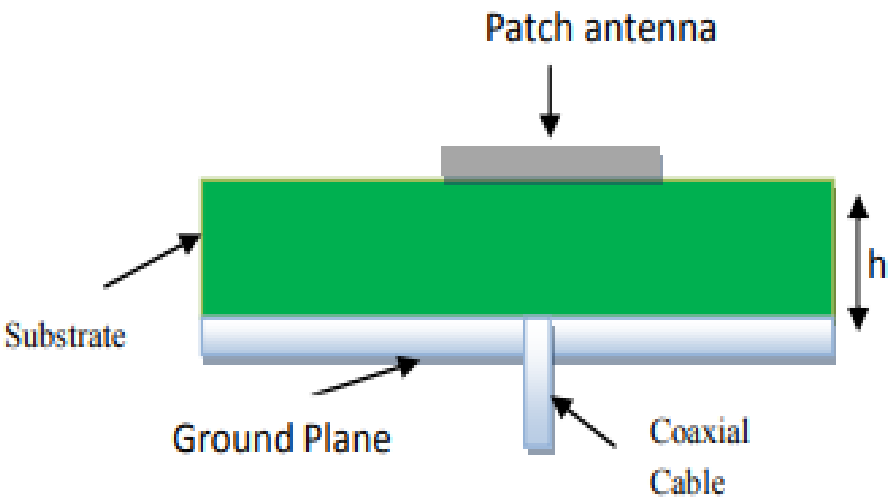

Figure 2. 10 Coaxial probe feed (Singh & Tripathi, 2011).

Because it is a simple conducting strip connecting to the patch and thus will be considered an extension of the patch, as shown in figure (2.5), the microstrip line feeding printing operation is one of the simplest ways to fabricate. It is simple to model and straightforward to match by dominating the inset position. However, as the thickness of the substrate rises, the amount of surface wave and spurious feed radiation increases, limiting the bandwidth (Singh & Tripathi 2011).

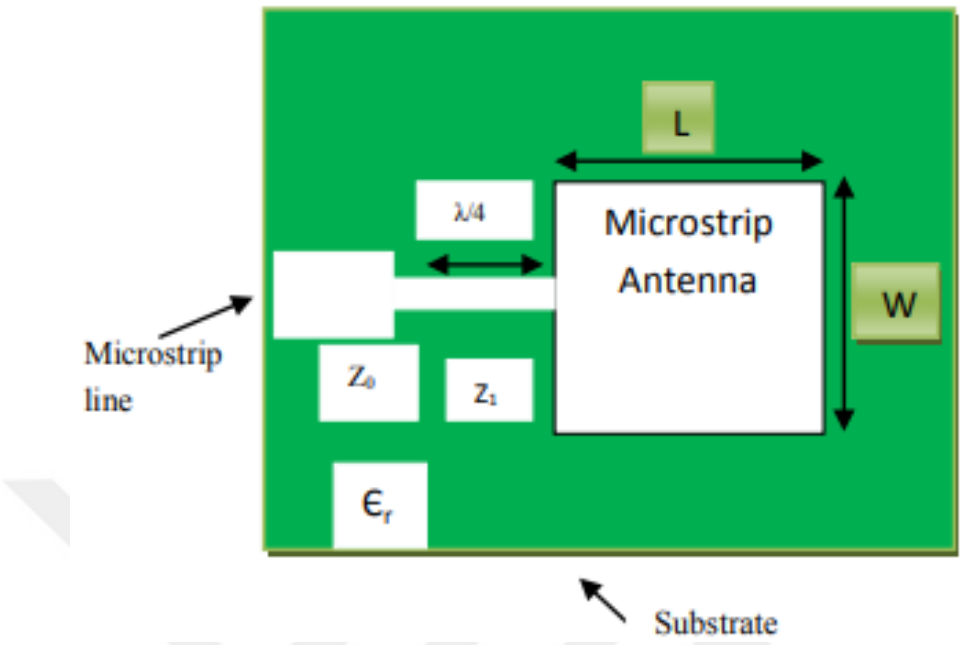

Figure 2. 11 Microstrip line feed patch antenna (Singh & Tripathi 2011)

An aperture-linked feed transports two completely distinct substrates separated by a ground plane. A microstrip feed line with a ground plane separates two substrates and is located on a very inexpensive facet of the bottom substrate. This configuration allows for the independent development of the feed mechanism and divergent components. The top substrate is usually a thick, low, nonconductor constant substrate, whereas the bottom substrate is typically a thick high, nonconductor constant substrate. The central ground plane isolates the feed from the radiation component and prevents radiation interference for pattern formation and polarization purity, allowing for unfettered optimization of the feed mechanism part (see figure) (2.16) (Singh & Tripathi 2011).

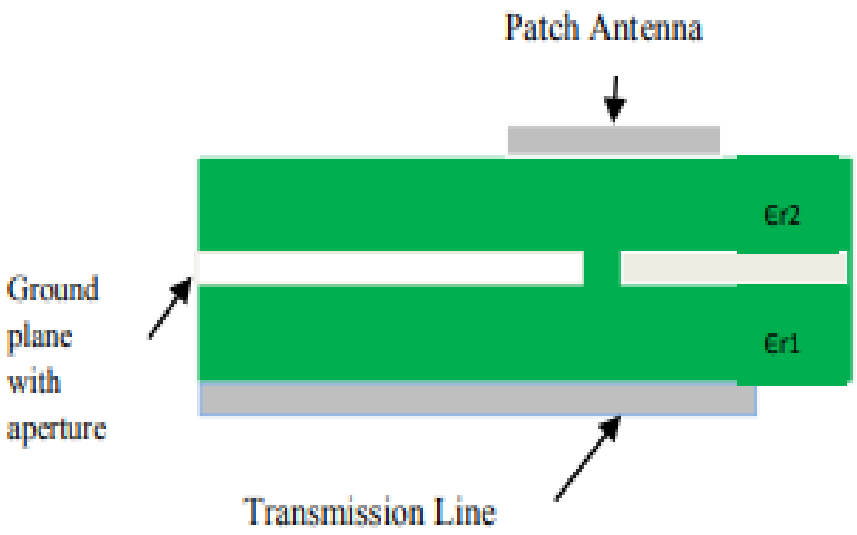

Figure 2. 12 Aperture coupled feed patch antenna (Singh & Tripathi 2011)

Proximity coupling has the most excellent bandwidth and emits the most negligible radiation. Manufacturing, on the other hand, remains a hurdle. Feeding the heel length and width to limit the length ratio of the patch. The coupling method is capacitive, as shown in figure (2.7).

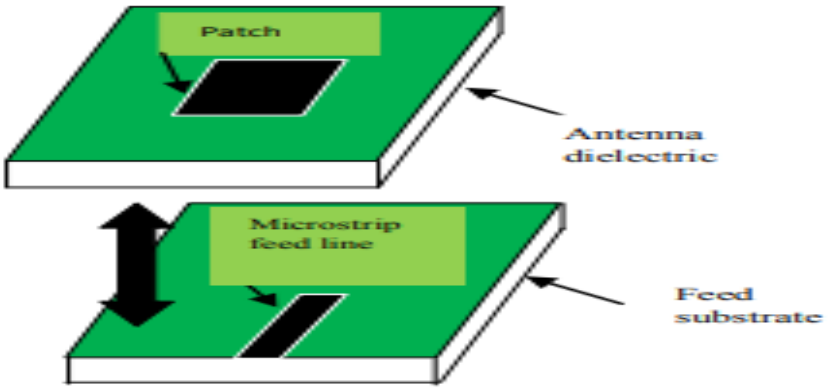

Figure 2. 13

Proximity coupling Microstrip patch antenna (Singh & Tripathi 2011)

2.7 Antenna Parameters

2.7.1 Quality Factor

A quality factor represents an antenna loss, a merit number. Radiation, conduction (ohms), dielectric, and surface wave losses are all standard. As a result, these losses impact the overall quality factor Q_t, commonly represented as approximate formulae to express the quality factors for various losses for fragile substrates of variable shapes (including rectangular and circular) [56]. It can be expressed to:

$$\frac{1}{Q_t} = \frac{1}{Q_{rad}} + \frac{1}{Q_c} + \frac{1}{Q_d} + \frac{1}{Q_{sw}} \qquad (2.1)$$

Q_t = total quality factor

Q_{rad}= quality factor due to radiation (space wave) losses

Q_c = quality factor due to conduction losses

Q_d= quality factor due to dielectric losses

Q_{sw}= Quality factor due to surface

2.7.2 Efficiency

The power radiated divided by the input power is the radiation efficiency of an antenna. It may also be expressed in terms of quality factors, which for a microstrip antenna are written as (C. Balanis, 1997)

$$e_{cdsw} = \frac{Q_t}{Q_{rad}} \qquad (2.2)$$

2.7.3 Polarization

The elliptical antenna polarized field. Linear associates in circular polarizations are examples of a conic obtained when the conic is transformed into a line or a circle. When the electrical field is clockwise (CW), it helps set the rotation of the electrical field vector and the direction of wave

propagation type; therefore, the correct screw is known as right PolarizationPolarization, whereas counter-clockwise (CCW) is known as left PolarizationPolarization. Typically, the PolarizationPolarization is resolved using a mixture of orthogonal PolarizationPolarization, co-polarization, and cross-polarization [57].

Linear PolarizationPolarization for the wave to have linear PolarizationPolarization, the time-phased difference between the two components must be

$$\Delta \varphi = \varphi_y - \varphi_x = n\pi,\ n = 0,1, 2, 3, \qquad (2.3)$$

Circular PolarizationPolarization is only possible when the magnitudes of the two components are the same, and the time-phase difference between them is an odd multiple of $\pi/2$. That is,

$$|E_x| = |E_y| \Rightarrow E_{x0} = E_{y0} \qquad (2.4)$$

$$\Delta \varphi = \varphi_y - \varphi_x = +(1/2+2n)\,\pi,\ n = 0, 1, 2, \cdots, \text{for CW} \qquad (2.5)$$

$$\Delta \varphi = \varphi_y - \varphi_x = -(1/2+2n)\,\pi,\ n = 0, 1, 2, \cdots, \text{for CCW} \qquad (2.6)$$

When the time-phased difference between the two components is odd multiples of 1/2, and their magnitudes differ, or when the time-phase difference between the two components is not multiples of $\pi/2$ (regardless of their magnitudes), elliptical PolarizationPolarization can be created (irrespective of their magnitudes) that is, when (D.-G. Fang, 2017; D. Fang, 2017)

$$\Delta \varphi = \varphi_y - \varphi_x = +\left(\frac{1}{2} + 2n\right)\pi,\quad n = 0, 1, 2, \cdots, \text{for CCW} \qquad (2.7)$$

$$\Delta \varphi = \varphi_y - \varphi_x = -\left(\frac{1}{2} + 2n\right)\pi,\quad n = 0, 1, 2, \cdots, \text{for CCW} \qquad (2.8)$$

Also, $|Ex| \neq |Ey| \Rightarrow Ex_0 \neq Ey_0$.

2.7.4 Gain

Gain within the coil antenna is the essential performance parameter. However, antenna gain may be measured or calculated. Furthermore, there has lately been a spike in interest in wireless applications. The accuracy criteria for estimating antenna gain have been raised. There are several basic formulae for determining gain. Every formula contains a different level of relevance, and erroneous application of those formulae might result in incorrect gain numbers. Gain (G) is directivity reduced by antenna construction losses [58].

$$\boldsymbol{G = e_r D} \tag{2.9}$$

G is the gain, e is efficiency, and D is the directivity**.**

2.7.5 Directivity

Directivity is the increase in power density in a specific direction at a certain distance from a transmitting antenna, compared to the power density with the same transmit power distributed uniformly in all directions. The maximum value of directivity is usually of substantial consequence; hence, directivity can be used to refer to maximal directivity. So, directivity measures the increase in maximum power density at a fixed distance in W/m^2 (Stutzman & Magazine 1998).

2.7.6 Antenna Bandwidth

Bandwidth is "the frequency range within which the antenna's performance in terms of some attribute adheres to a specified standard." The bandwidth consists of the frequencies to the left and right of a signal's central frequency (generally the resonant frequency). The antenna's performance conforms to industry standards. The impedance bandwidth of an antenna is defined as the power supplied to the antenna that exceeds 90 percent of the available power. The prism of reflection is another method for analyzing antenna bandwidth. The coefficient describes the relationship between two variables. Frequently, the equation is used to plot the power reflection coefficient where the minimum reflection coefficient is less than -10 dB (Jafarian, Kashani-Bozorg, Amadeh, & Atassi, 2021).

$$|\Gamma|_{dB} = 20\log_{10}|\Gamma| = 10\log_{10}|\Gamma|^2 \qquad (2.10)$$

$$\Gamma = \frac{z_a - z_o}{z_a + z_o} \qquad (2.11)$$

Z_o is the line impedance and corresponds to the generator resistance, typically 50. Z and is the radiation resistance of the antenna. Ninety percent of the available power to the antenna is delivered when the power reflection coefficient is -10dB. The graph in the Figure 2.19 depicts the reflection coefficient in terms of frequency (Fung 2011).

The X-axis represents the

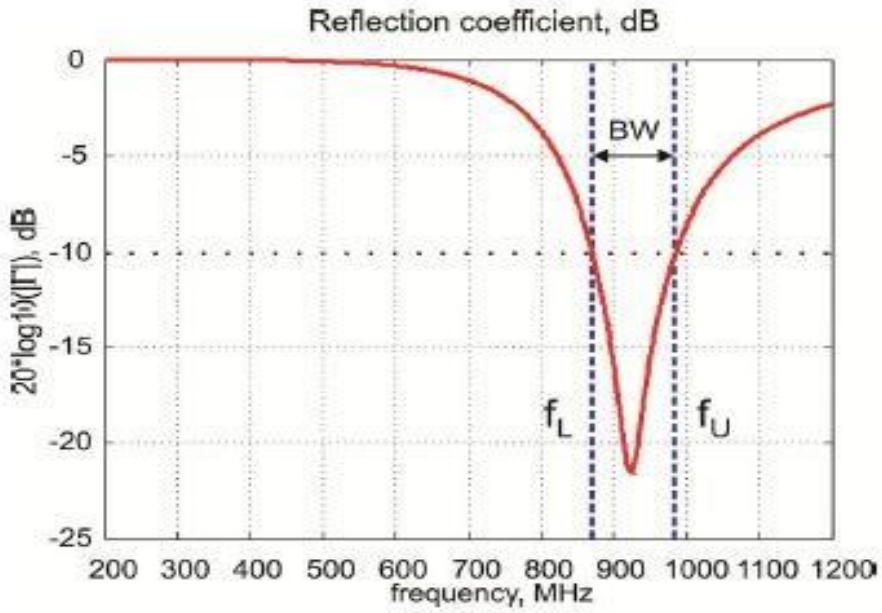

the y-axis represents the return loss in

Figure 2. 14 The reflection coefficient in terms of frequency (Fung 2011)

(f_L) denotes the lowest frequency at which 90 percent power is satisfied, while (fU) represents the most significant frequency. The average of (f_l) and (f_U) will give you the center frequency fc, and the bandwidth, commonly referred to as fractional bandwidth, is determined by equation(2.12).

$$\text{Fractional Bandwidth} = \frac{f_u - f_L}{f_L} \times 100\% \qquad (2.12)$$

2.7.7 Substrate of Patch Antenna

The size of the microstrip antenna is influenced by the substrate's dielectric constant. The substrate slows the propagating wave through the substrate with a greater dielectric constant, making the wave radiating elements smaller. This means the elements are built for a greater frequency, but the antenna will operate at a lower frequency due to the dielectric constant. In addition, patch antennas can be susceptible to interference at specific frequencies, with substrate Flame Resistant (FR4) being a low-cost substrate purchased in sheets. The thicker it is, the higher the cost of the substrate material.

Furthermore, Plexiglas is a less lossy material than FR4, improving overall efficiency. FR4 and Plexiglas are less expensive than Teflon sheets. Teflon sheet is more expensive than FR4 and Plexiglas, as shown in Table (2.1) shows substrate materials (Fung 2011).

Table 2. 2 Substrate Materials

Substantial	Rate	Dielectric Constant
FR4	Cheap	4.35 – 4.7
Plexiglas	Medium Cost	2.6 – 3.5
Teflon	Expensive	2.1

CHAPTER THREE

PROPOSED ELLIPTIC PATCH UWB ANTENNA

3.1. Antenna Patch

The "Federal Communication Commission" in the United States has approved the use of UWB technology in frequency ranges between (3.1 to 10.6 GHz), and the tiny size and reduced cost are the main research targets in "commercial" and "military" applications. Ultra-wideband technology for wireless systems frees users from wires and allows them to link many devices and multiple users wirelessly in dispatch and reception. This chapter proposed a 16×12 mm^2 elliptical slot Ultra-wideband (UWB) printed monopole microstrip antenna. The coaxial connector of the SMA has been excited with the design of the compact, thin, and planar UWB antenna, which contains two elliptical slot radiators that are supplied with one 50 micro-strip lines with the reduced ground plane.

3.2. Proposed Elliptic Patch Antenna

For analysts and engineers, ultra-wideband antenna design has become a fascinating topic. The "UWB" communications offer various applications and areas of interest. With three notched bands of 4.3 GHz (Wi-Fi band), and 11.7 GHz (WLAN band), this suggested antenna has a very high bandwidth from 3.62 to 13.78 GHz, as defined by the voltage standing wave ratio VSWR 2. The dimensions of the elliptic UWB antenna shown in Figure (3-1) are 16 mm × 12 mm (L × W). This elliptical antenna is made up of several small designs that are intended to acquire frequencies in the UWB band. The tiny antenna is printed on the face of a 1.6 mm thick FR-4 substrate with a relative permittivity of 4.3. Using the CST Studio computer application, an antenna execution has been analyzed in terms of "S-parameter," "largest gain," "radiation proficiency," and "radiation design" features in each working condition.

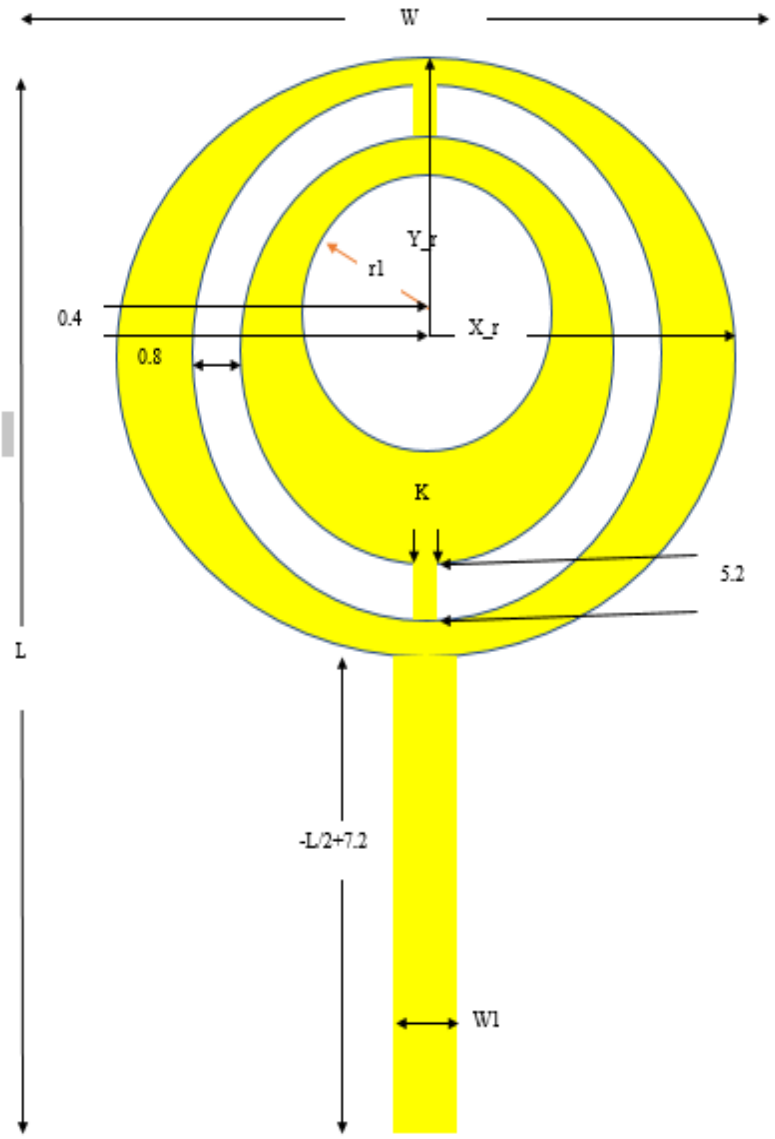

(a)

(b)

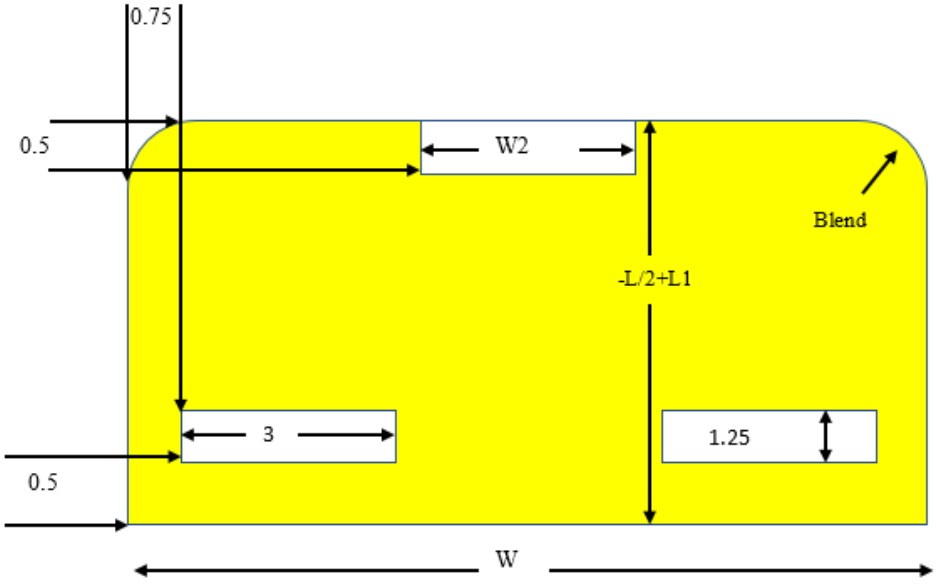

However, the resonant length of a microstrip patch can be determined using simple, effective relative dielectric constant relationships as an operating frequency and substrate characteristics function, as shown below:

Figure 3. 1 Proposed Elliptic Patch UWB Antenna

(a) Front view (b) Back view

$$\varepsilon_{reff} = \frac{\varepsilon_{reff}+1}{2} + \frac{\varepsilon_{reff}-1}{2}\left[1+12\frac{h}{W}\right]^{\frac{-1}{2}} \quad (3.1)$$

$$W = \frac{c}{2f}\sqrt{\frac{2}{\varepsilon_r+1}} \quad (3.2)$$

$$L_{eff} = \frac{c}{2f\sqrt{\varepsilon_{reff}}} \quad (3.3)$$

$$\Delta L = 0.5h \quad (3.4)$$

$$L = L_{eff} - 2\Delta L \quad (3.5)$$

Where c denotes the speed of light in free space, L denotes the length of resonant patch antennas, and W denotes the width of resonant patch antennas. The suggested antenna parameters are listed in Table (3-1) below:

3.2.1. Parametric Analysis of Elliptic Patch Antenna Proposed

The geometric parameters significantly impact an antenna's performance; hence, this part presents a parametric study of an elliptical patch ultra-wideband antenna. A design curve for the feed transmission line, ground plane, and slot dimensions has been produced for various band frequencies. The variety of bandwidth has also been considered, as well as the proportion of these layouts. The degree of bandwidth and radiation designs of these arrangements have been tested, and the results match the simulated results.

a. Substrate Length Effect (L)

As a first parameter, the substrate length shown in Fig. (3-2) was simulated; this figure depicts the simulation of the "S-parameter" over various substrate length values. The curve shows that (L = 16 mm) provides the best bandwidth between (3.6 and 13.7) GHz, with a reflection coefficient of S11≤ dB.

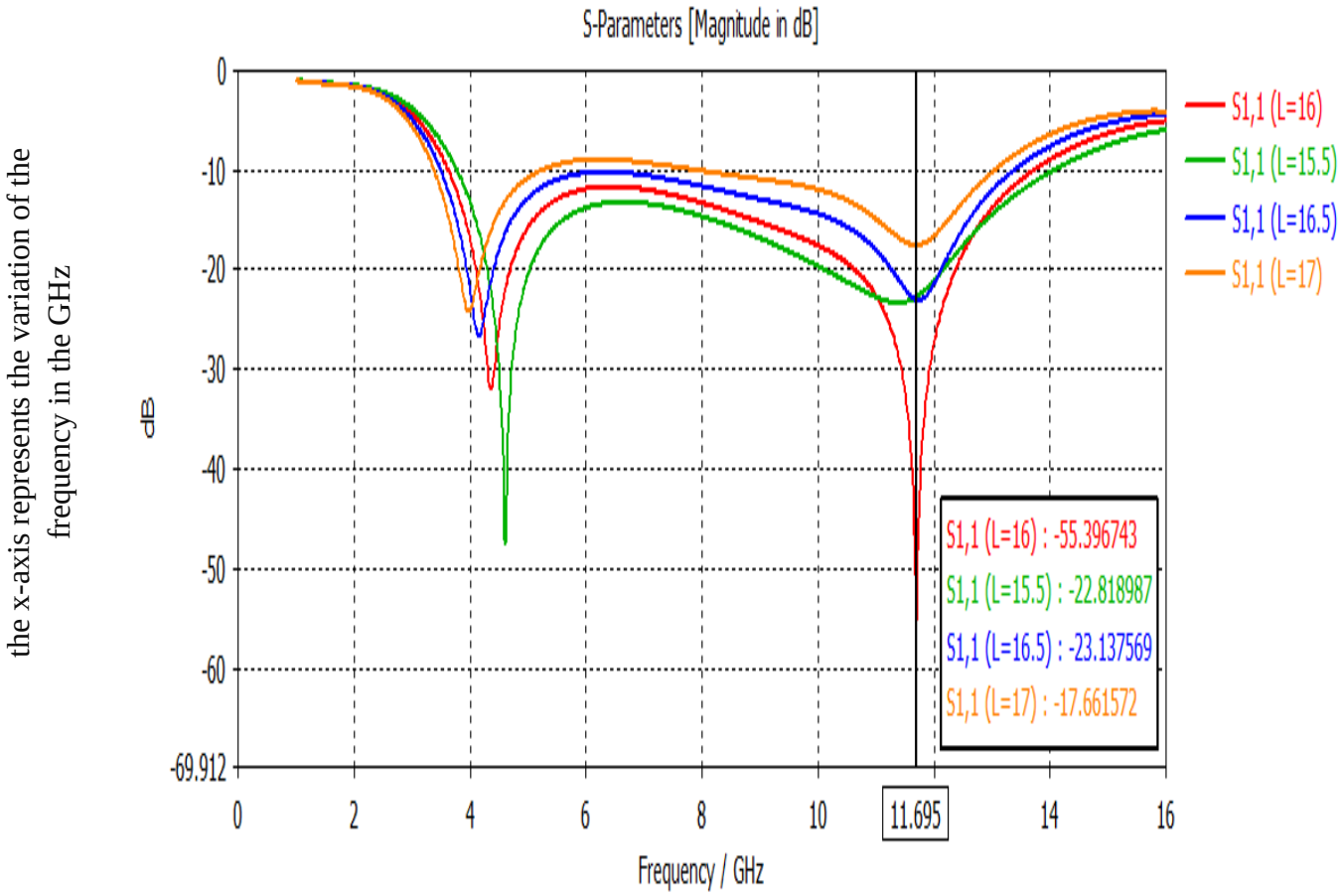

Figure 3. 2 S-parameter of an elliptic patch antenna value (L).

b. Effect of Substrate width (W)

The substrate width was simulated as a second parameter. The simulated "S-parameter" for various values of substrate width is shown in Fig. (3-3). From the curve, it can be noticed that (W = 12 mm) gives preferable bandwidth from (3.6 to 13.7) GHz with a reflection coefficient $S11 \leq -10$ dB.

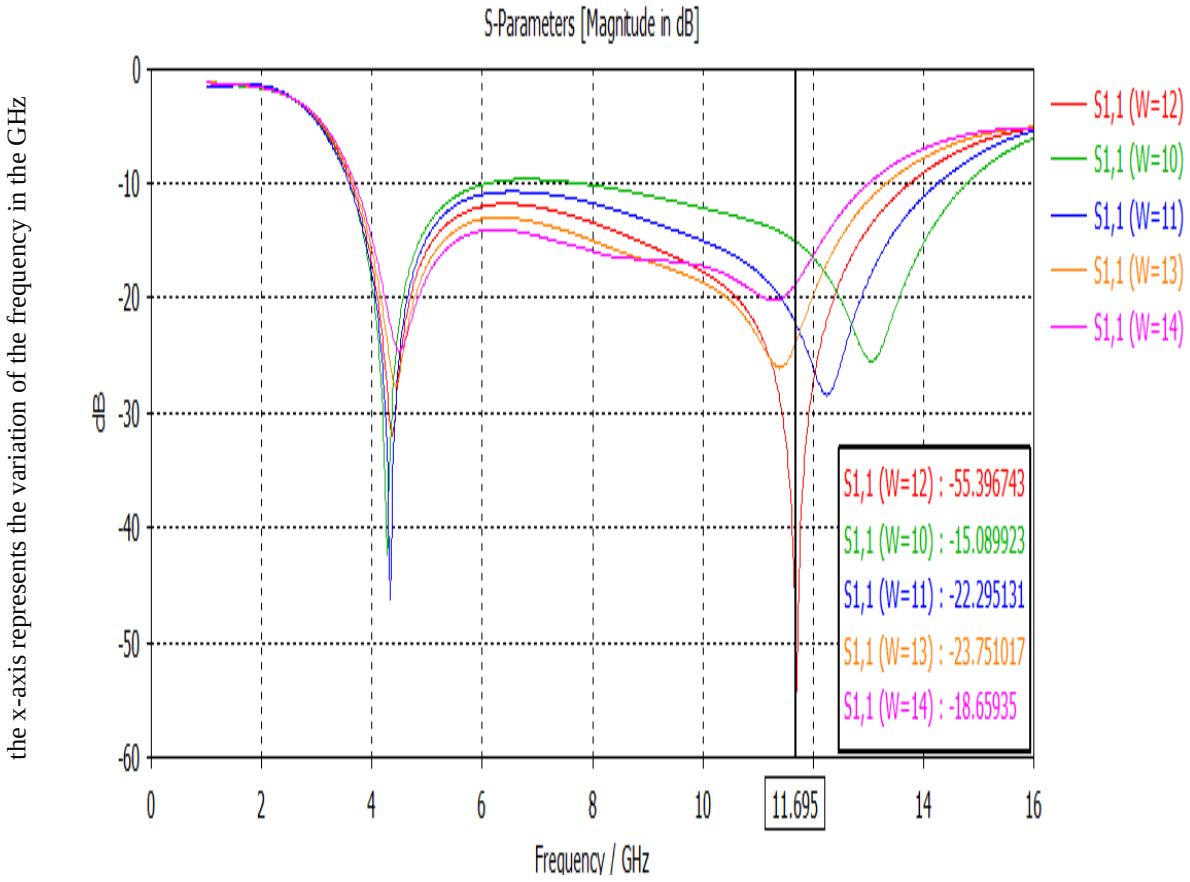

Figure 3. 3 S-parameter against frequency for various values of (W)

c. The width of a rectangular hole in the antenna's ground (W2) effect.

The sixth parameter simulated is the width of the square hole in the antenna's ground, shown in Fig. (3-4). This figure illustrates the simulation of the "S-parameter" for various values of the width of the square hole in the antenna's ground. From the curve, it can be observed that (W2 = 2 mm) gives the best bandwidth from (3.6 to 13.7) GHz with a reflection coefficient of $S11 \leq -10$ dB.

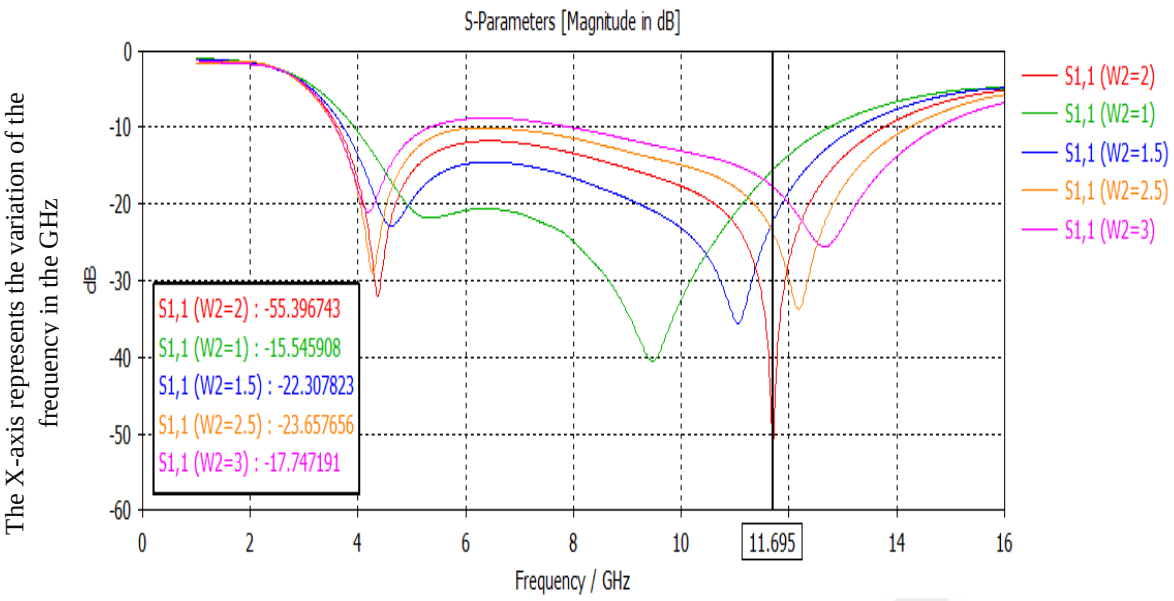

Figure 3. 4 S S-parameter of an elliptic patch antenna versus various values of (W2)

d. The effect of the center circle's radius (**r1**)

The fourth parameter simulated is the radius of the center circle. The simulated "S-parameter" for diverse values of the center circle's radius is shown in Fig. (3-5). From the curve, it can be noticed that (r1= 2 mm) gives preferable bandwidth from (3.6 to 13.7) GHz with a reflection coefficient $S11 \leq -10$ dB.

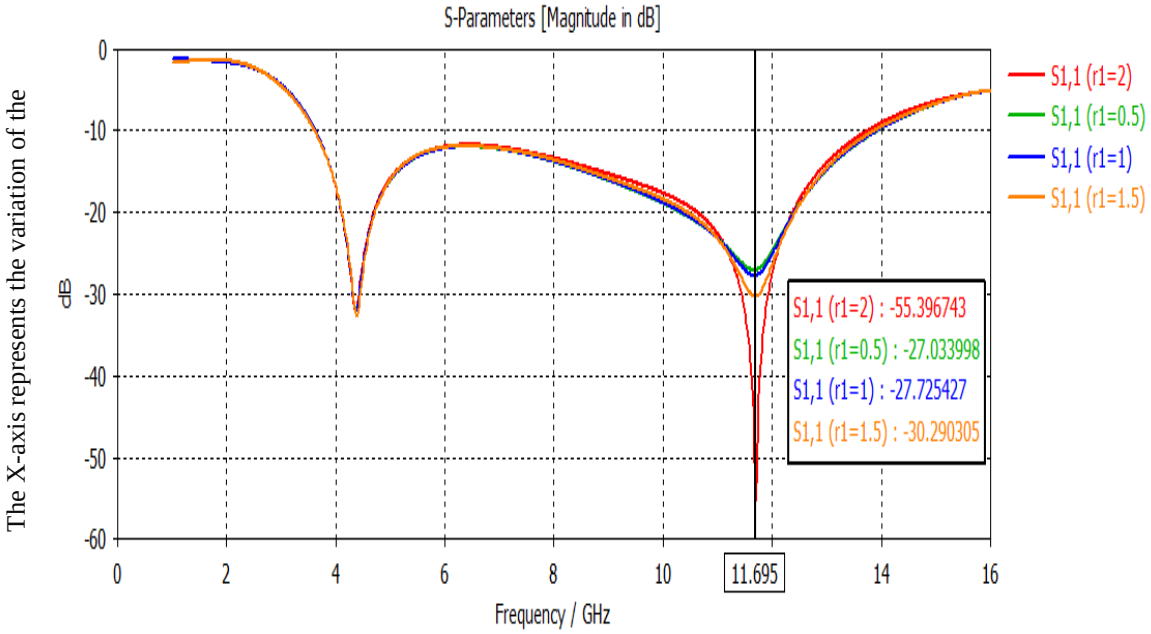

Figure 3. 5 S-parameter simulation for an elliptic patch antenna value of (r1)

e. Effect of the width of the antenna patch in the elliptical shape (K)

The fifth parameter simulated is the width of the rectangular shape in the ellipse. The simulated "S-parameter" for diversified values of the center circle's radius is shown in Fig. (3-6). From the curve, it can be noticed that (k = 0.2 mm) gives a preferable bandwidth from (3.6 to 13.7) GHz with a reflection coefficient of $S11 \leq -10$ dB.

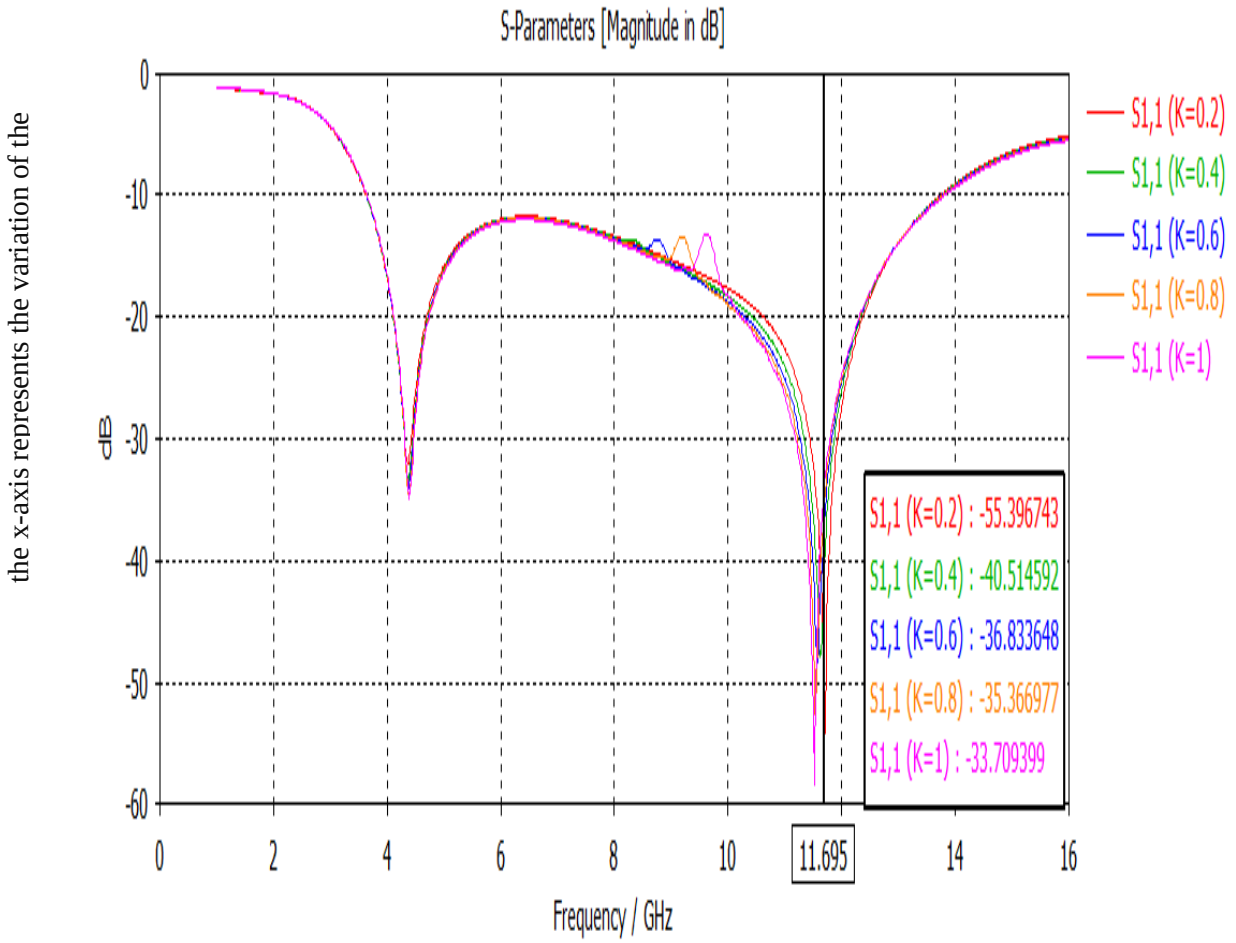

Figure 3. 6 S-parameter simulations for an elliptic patch antenna (k) value.

f. Effect of X-Axis radius of the ellipse shape (**X_r**)

The "X-Axis" radius of an ellipse shape, shown in Fig. (3–7), was simulated as a third parameter. This figure illustrates the simulation of the "S-parameter" for assorted values of the X-Axis radius of the ellipse shape. From the curve, it can be observed that (Xr = 5 mm) gives preferable bandwidth from (3.6 to 13.7) GHz with a reflection coefficient of$S11 \leq -10$ dB.

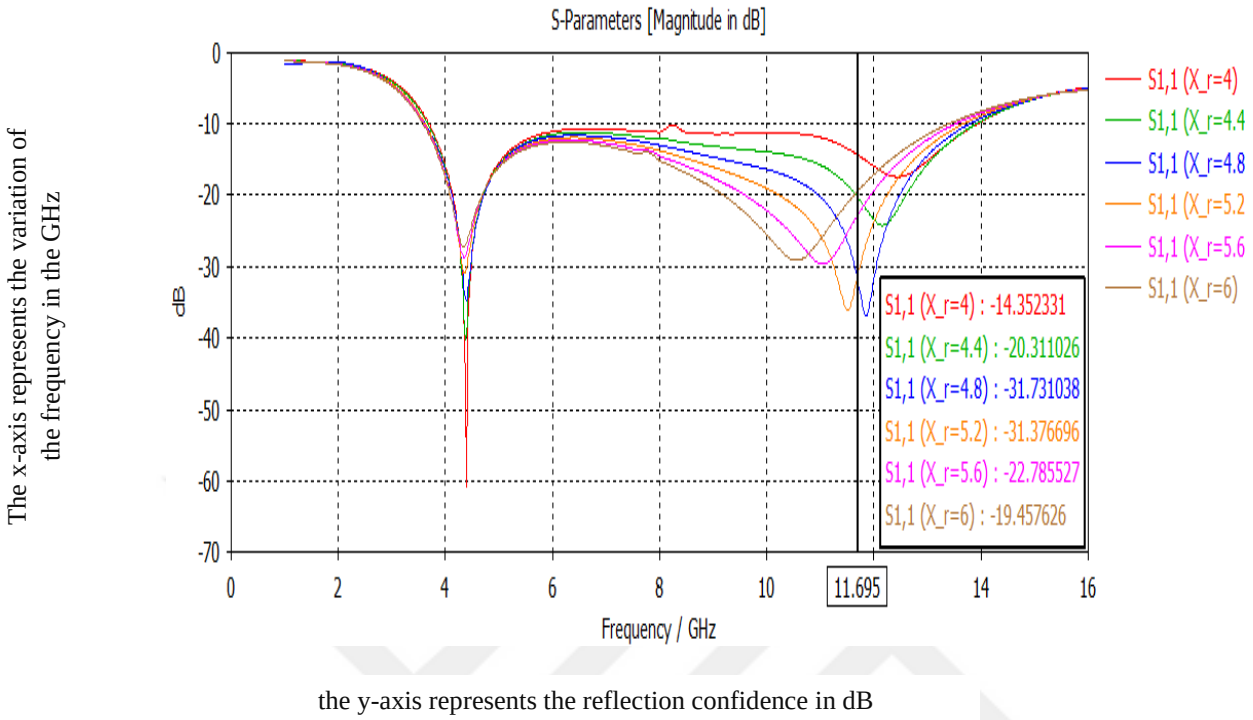

Figure 3. 7 S-parameter simulation for an elliptic patch antenna at various (X r) values.

g. Effect of Y-Axis radius of the ellipse shape ($\boldsymbol{Y\_r}$)

The seventh parameter simulated is an ellipse shape's "Y-Axis" radius. The simulated "S-parameter" for diverse values of the "Y-Axis" radius of the ellipse shape is shown in Fig. (3-8). From the curve, it can be noticed that (Yr = 4.6 mm) gives a preferable bandwidth from (3.6 to 13.7) GHz with a reflection coefficient of$S11 \leq -10$ dB.

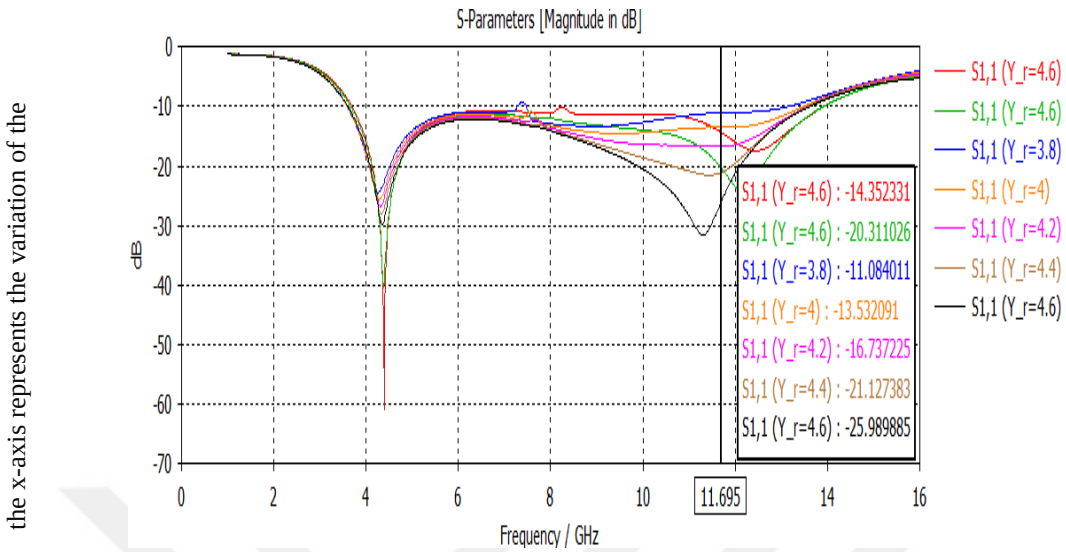

Figure 3. 8 Simulation of the S-parameter for an elliptic patch antenna at various (Y r) values

h. Effect of C width

The last parameter simulated is "C" with a rectangular cut in the ground of the proposed antenna. The simulated "S-parameter" for diverse values of "C" width of the rectangular cut is shown in Fig. (3-9). From the curve, it can be noticed that (C = 2 mm) gives preferable bandwidth from (3.6 to 13.7) GHz with a reflection coefficient of $S11 \leq -10$ dB.

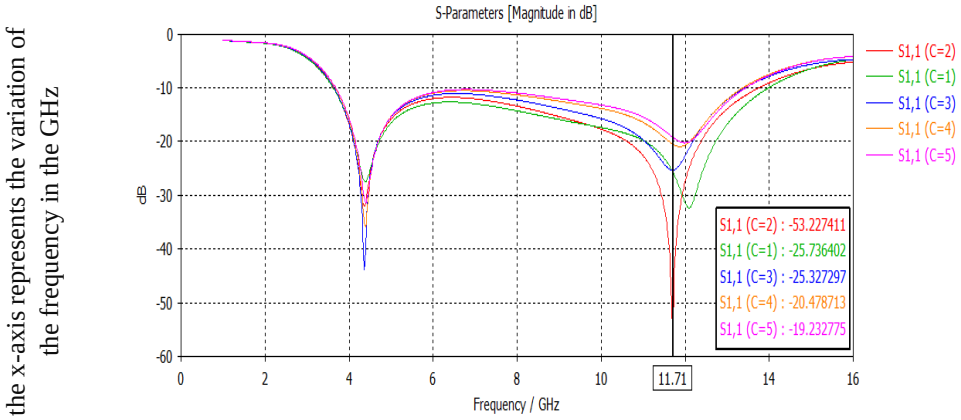

Figure 3. 9 Simulation of the S-parameter for a rectangular incision in the antenna ground

3.2.2. Characteristics of an Elliptic Patch antenna

This section describes the characteristics of the suggested antenna with the best parameter values. As shown in Table

Table 3. 1 Detailed Parameter for the Proposed Elliptical Patch Antenna

No.	Symbol	Definition	Size (mm)
1	L	Substrate length	16
2	W	Substrate width	12
3	L_1	The length of the antenna ground	4.4
4	W_1	Feeder width	4.4
5	W_2	Width of the rectangular slot on the ground	2
6	r_1	The radius of the center circle	2
7	Blend	Blend of the ground edges	2
8	K	Width of the antenna patch in the Elliptical Shape	0.2
9	X_r	X-Axis radius of the Elliptical Shape	5
10	Y_r	Y-Axis radius of the Elliptical Shape	4.6
11.	C	Width of the rectangular cut in the ground	2

a. Gain of the Antenna

When simulated, the suggested elliptic patch antenna' gain appears in Fig. (3-10). This curve shows that the most extreme gain, equal to 3.5 dB, can be accomplished at (11.5 GHz) while the minor gain is equal to -6 dB at (2 GHz).

the x-axis represents the variation of the

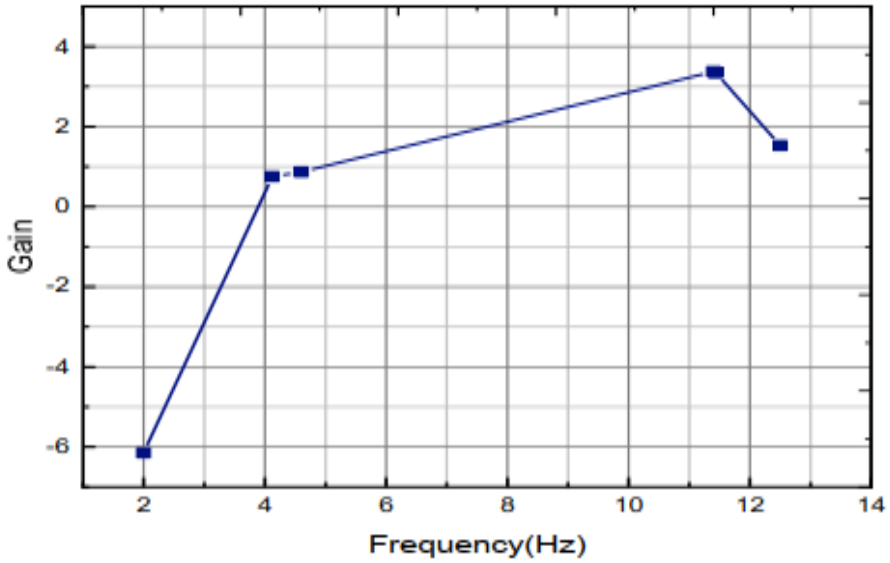

Y-axis represents the gain.

Figure 3. 10 Antenna Gain b. S-parameter

The proposed antenna's simulated and measured S-parameter covers are plotted as shown in Fig. (3-11). In this figure, you will notice that the proposed antenna achieves a bandwidth of (3.6 to 13.7) GHz. This band is beneficial for many applications that can be used in civil, military, and government organizations for weather monitoring, defense tracking, vehicle speed detection, Etc.

It is clearly shown that the bandwidth of the proposed antenna is equal to 10.16 dB with an of-56.299 dB.

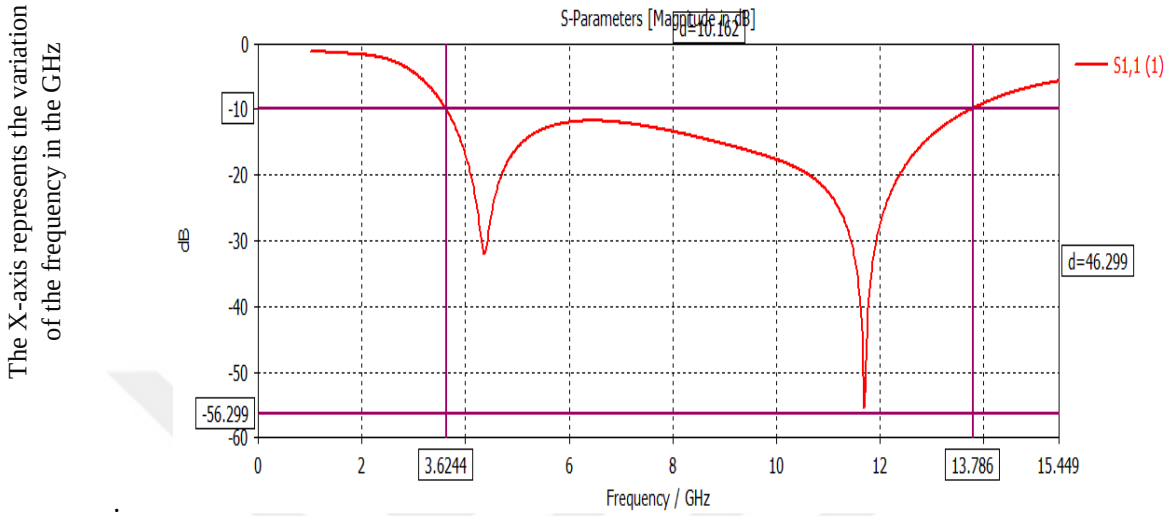

Y-axis represents the reflection confidence in dB.

Figure 3. 11 S-Parameter simulation vs. frequency for an elliptical patch antenna

c. "Voltage Standing Wave Ratio" (VSWR)

Fig. (3-12) explains VSWR against the frequency of the suggested antenna. From the curve, it is observed that the value of VSWR is acceptable at the entire achieved band.

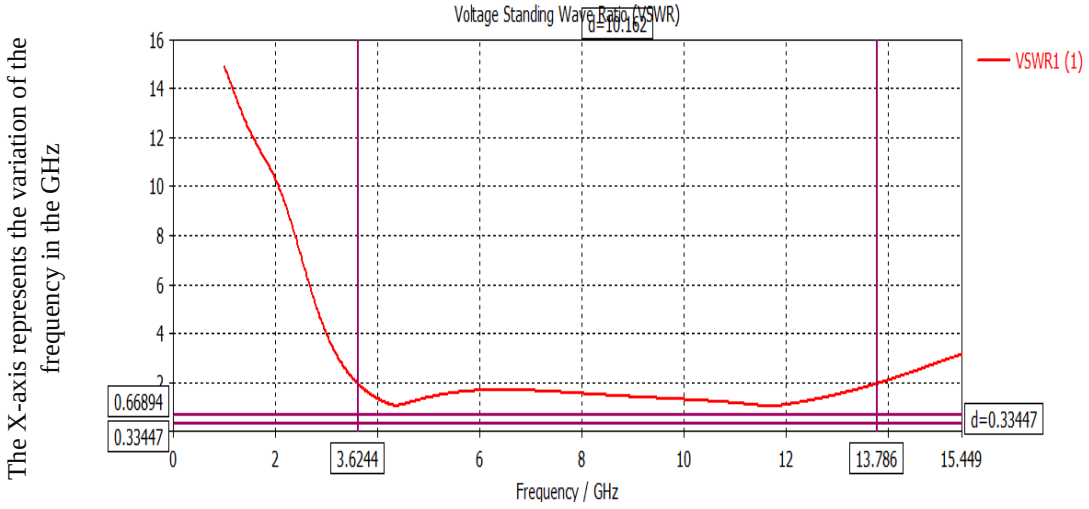

Y-axis represents the VSWR.

Figure 3. 12 An elliptical patch antenna's VSWR vs. frequency simulation

d. Input Impedance

Fig. (3-13) illustrates the impedance variation of the real part and imaginary part with frequency.

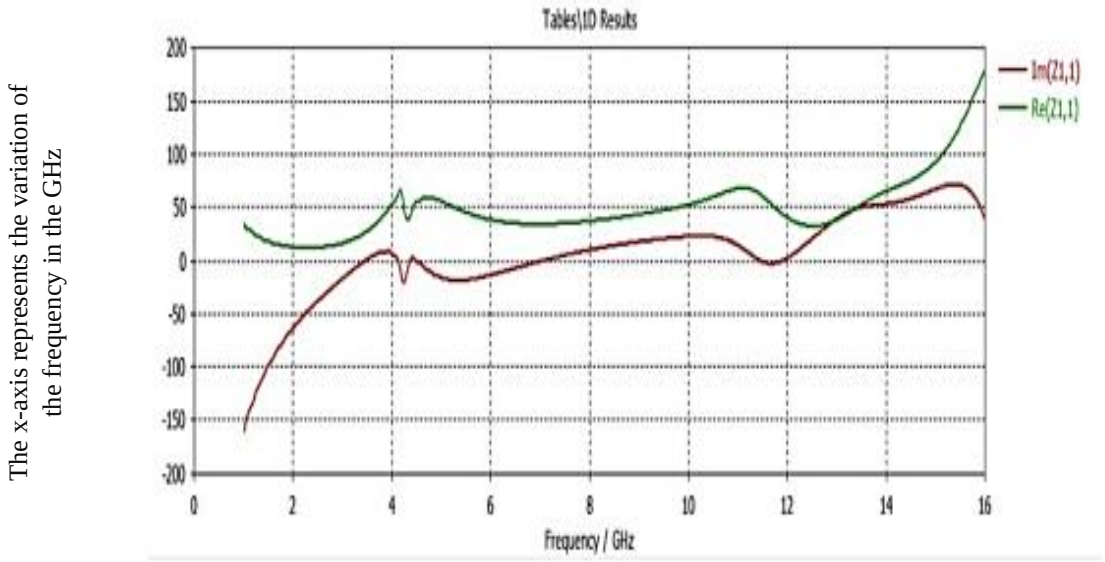

Figure 3. 13 Proposed antenna input impedance

e. Current Distribution

The current distribution of the suggested antenna is shown in Fig. (3-14) at frequencies (4.3 and 11.7) GHz. At frequency (4.3 GHz), Fig. (3-14, a) explains that the maximum current is equal to (187.085 A/m); at a frequency (11.7 GHz), Fig. (3-14, b) explains that the maximum current is equal to (186.799 A/m).

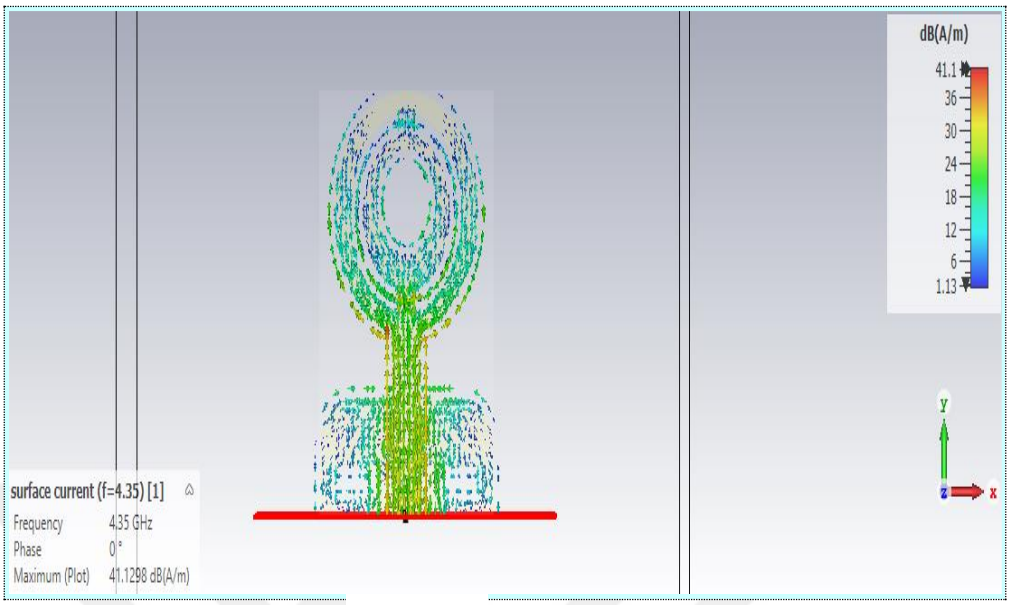

(a)

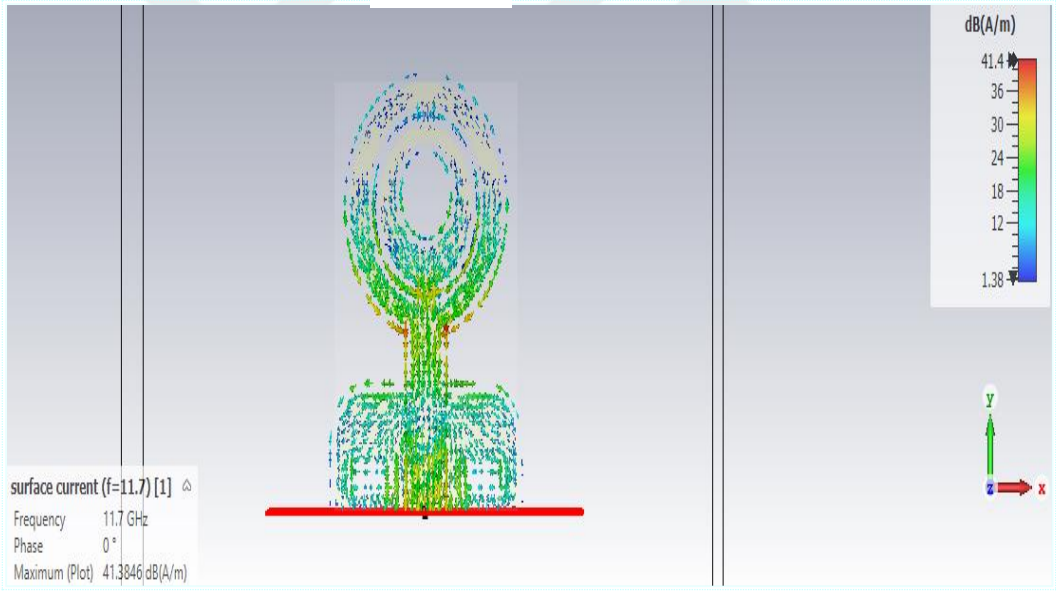

(b)

Figure 3. 14 Current frequency distributions at (a) 4.3 GHz and (b) 11.7 GHz.

f. 3D Radiation Pattern

The 3D radiation for frequencies of 4.3 GHz and 11.7 GHz will be illustrated in Fig. (3-15). In this figure, it can be observed that the radiation pattern at 4.3 GHz has a maximum directivity of

3.14, and at 11.7 GHz has a maximum directivity of 3.13 dB. These designs have large, accomplished bandwidth properties required for numerous applications.

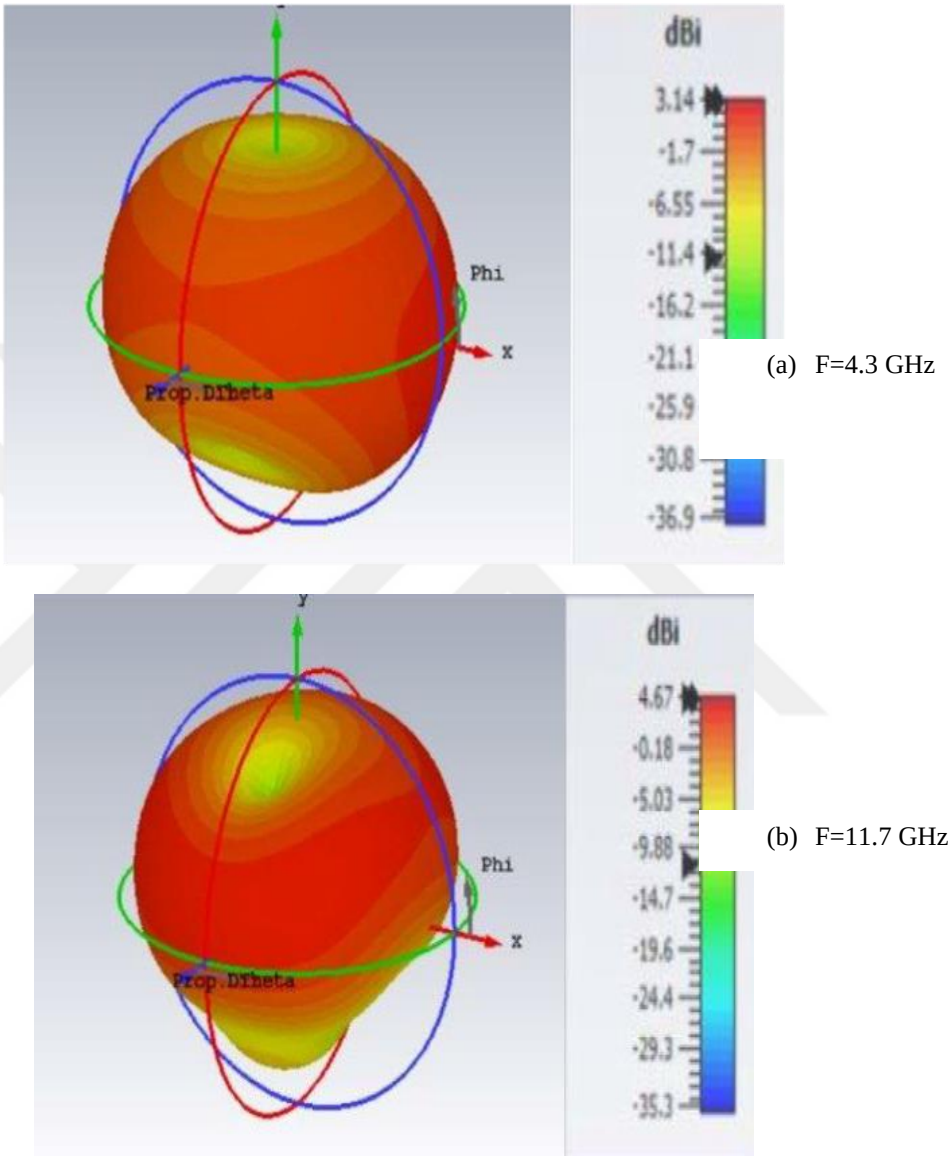

Figure 3. 15 a 3-D radiation pattern for an elliptic patch.

3.3. Far filed Radiation Patterns

Radiation patterns simulation of the improved antenna in the "y-z" plane (Electric -plane) and "x-z" plane (Magnetic-plane) for two frequencies through the passband, which equal to (4.3 and 11.7)."Fig. (3-16, a) presents (Electric -filed) and (Magnetic -filed) at 4.3 GHz, for (Phi=90) E-filed, has a primary lobe magnitude of 15.5◦ (dB in the direction) 159.0°(and angular width (3dB)

is (106.0◦), the Magnetic -filed has a primary lobe magnitude of (-36) dB in the direction (159.0◦) and angular width (3 dB) is (106.0◦). Fig. (3-16, b) illustrates the Electric -plane and Magnetic -plane at 4.3 GHz, for (Phi=90). The Electric -field has a primary lobe magnitude of (15.6) dB in the direction of (155.0°), and angular width (3dB) is (110.7◦). The Magnetic -field has a primary lobe magnitude of (-35.9) dB in the direction (155.0◦), and an angular width (3 dB) is (110.7◦).

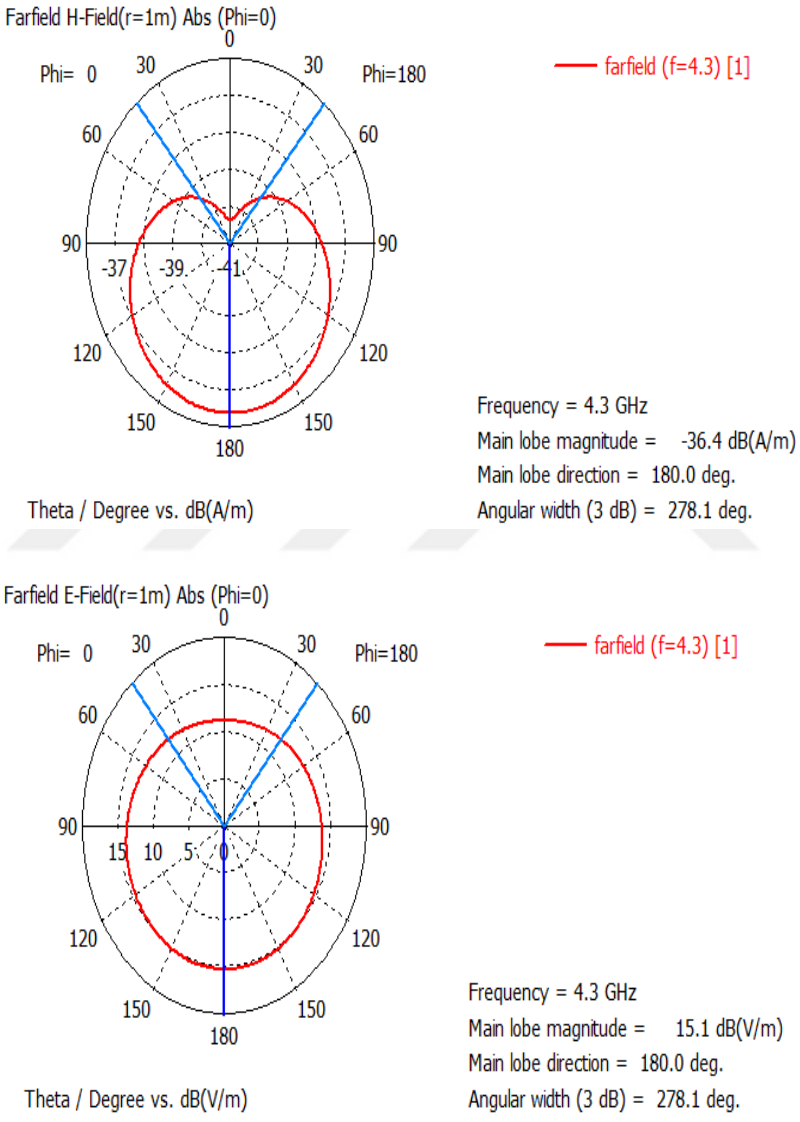

(a)

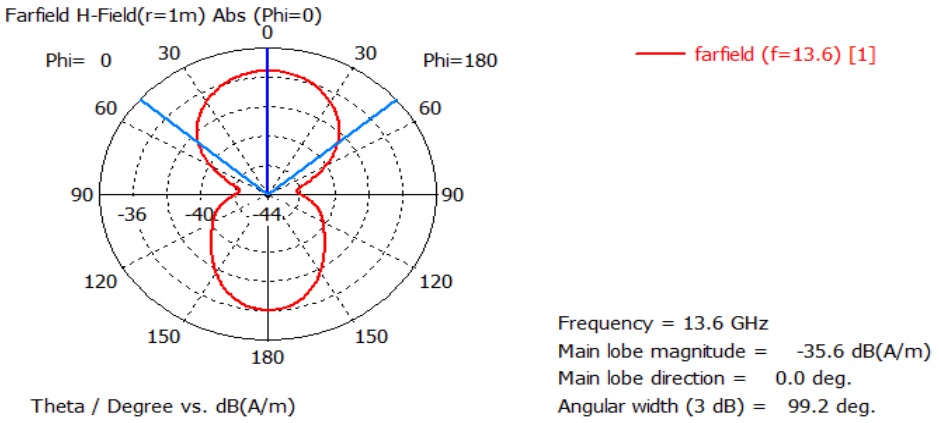

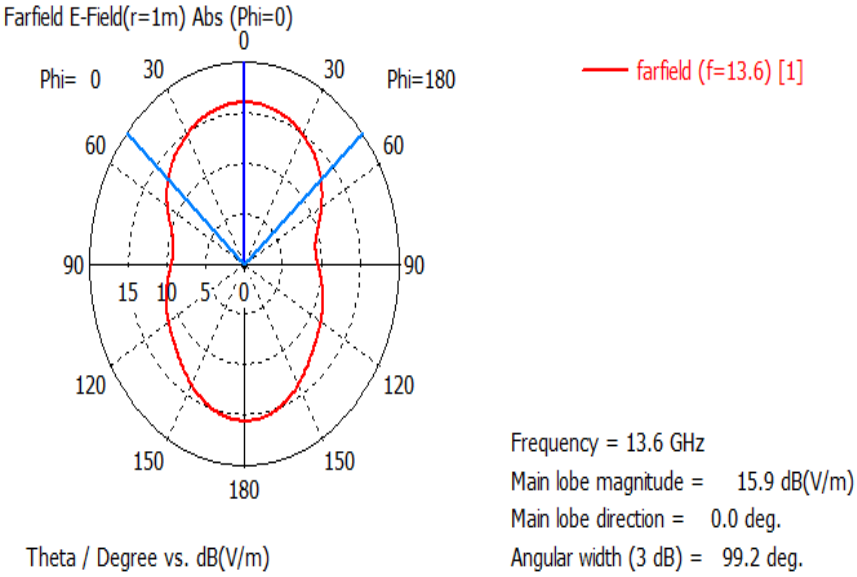

(b)

Figure 3. 16

(a) 4.3 GHz and (b) 11.7 GHz far filed patterns

3.4 Manufacturing of the Proposed Antenna

In this part, the CST suit findings of the proposed antenna are compared with accurate measurements to establish the design's validity. The manufacturing antenna results presenting in Figure.3.14, Elliptic Patch Antenna (The Front of The Antenna), and the Elliptic Patch Antenna (The Back of The Antenna.) are presented in figures 3.14 a and b, respectively. While the Figure 3.14.c representing the proposed antenna measure

.

(a)

(b)

(c)

Figure 3. 17 Manufactured Elliptic Patch Antenna

CHAPTER FOUR

PROPOSED SEMI-RECTANGULAR PATCH UWB ANTENNA

4.1. Rectangular Patch UWB Antenna

This chapter presents a semi-rectangular patch Ultra-wideband (UWB) antenna for Wi-Fi and WiMAX antenna applications. The measured radiation exhibitions of the suggested antenna are about an omnidirectional design in (H-plane) and a bi-directional design in (E-plane) for all the frequencies within the entire UWB band. The improvement handle of an antenna and its radiation properties are analyzed and discussed.

4.2. Proposed Semi-Rectangular Micro Strip Patch Antenna

This section describes the UWB semi-rectangular microstrip antenna design calculations and stage technique. The suggested antenna is 17.2 mm × 29.133 mm in size and is designed on an FR-4 substrate with a relative permittivity of 4.3 and a height of 1.6 mm. This suggested antenna has a wide frequency bandwidth ranging from 28 to 60 GHz, represented by the voltage standing wave ratio VSWR < 2, and two notched bands along the. The transmission line and the radiating patch of the U slot relate to tapered edges to provide more effective impedance matching. The proposed semi-rectangular microstrip antenna's parameters will be shown below in Fig. (4-1).

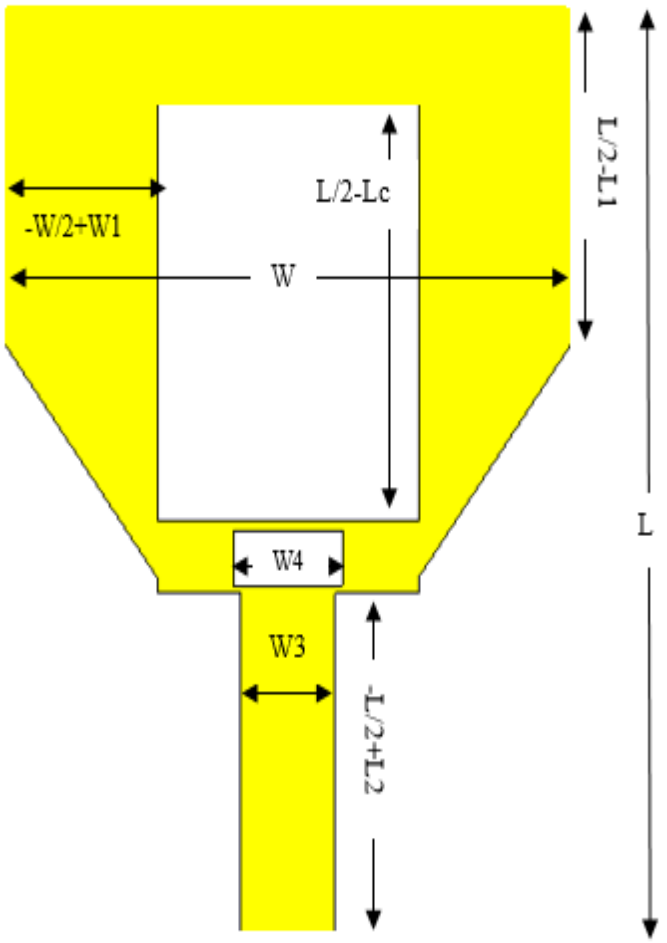

(a)

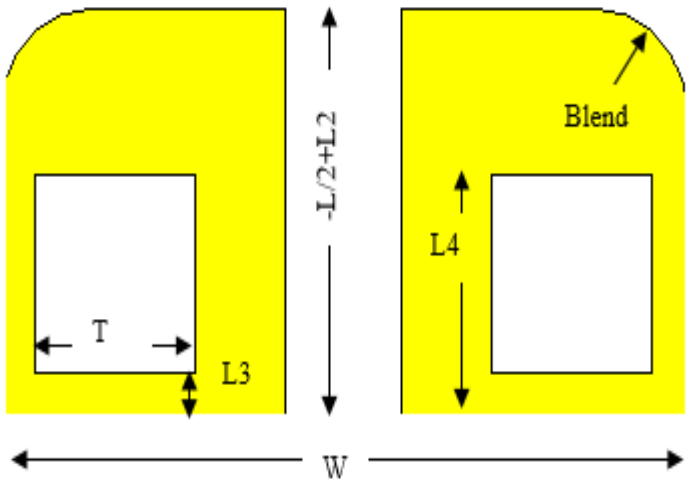

Figure 4. 1 (a) Front view (b) Back view of the proposed semi-Rectangular Patch UWB Antenna

4.2.1. Design Steps of Semi-Rectangular Patch Antenna

A 9.2 mm extended portion of the ground plane was used on the opposite substrate's side. It incorporates a 3.2□□×9.2□□ slot just behind the transmission line to improve bandwidth. The resonant length of a microstrip patch may be calculated using essential effective relative dielectric constant relationships as an operating frequency and substrate characteristics, as shown below:

$$\varepsilon_{reff} = \frac{\varepsilon_{reff}+1}{2} + \frac{\varepsilon_{reff}-1}{2}\left[1 + 12\frac{h}{W}\right]^{\frac{-1}{2}} \quad (4.1)$$

$$W = \frac{c}{2f}\sqrt{\frac{2}{\varepsilon_r+1}} \quad (4.2)$$

$$L_{eff} = \frac{c}{2f\sqrt{\varepsilon_{reff}}} \quad (4.3)$$

$$\Delta L = 0.5h \quad (4.4)$$

$$L = L_{eff} - 2\Delta L \quad (4.5)$$

Where c represents the light speed in free space, L represents the length, and W represents the width of resonant patch antennas. Some changes to this patch have been recommended in order to improve its working bandwidth. The initial adjustment was to trim the patch towards the micro-feeding strip's line. Due to the tapering effect of the component coupled to the micro-strip line, simulations have been used to modify the patch dimensions, as shown in Table 1. The patch length has been adjusted to 29.133 mm, and the patch width has been modified to 17.2 mm (4-1). Using those dimension values shows that the proposed antenna has a bandwidth (VSWR less than 2) between 28 GHz and 60 GHz, which covers the UWB band. Therefore, the proposed antenna is an excellent candidate for 5G applications.

.

4.2.2. Parametric Study of Proposed Semi-Rectangular Patch Antenna

A parametric study on different design parameters which influence the electrical execution of an antenna is done to attain the specified frequency range of UWB. Since the introductory parameters of the antenna do not grant the optimum result, an attempt to improve the performance is achieved by varying the parameters and then selecting the one which is the best.

An antenna's geometric parameters significantly impact its performance; therefore, this section presents a parametric study of a semi-rectangular alpha patch ultra-wideband antenna design curve for the feed transmission line dimensions, ground plane dimensions, and slot dimensions have been produced for various band frequencies. The variety of bandwidth has also been considered, as well as the proportion of these layouts. The degrees of bandwidth and radiation designs of these arrangements have been tested, and the results match the simulated results.

a. Substrate Length Effect (L)

The length of a substrate is simulated as the first parameter. Fig. (4-2) presents the influence of changing the length of the substrate on the S-parameter. When looking at the curve, it can be noticed that the substrate length (L=29.133 mm) gives preferable bandwidth from (28 GHz) to (60 GHz) with a reflection coefficient $S11 \leq -10$ dB.

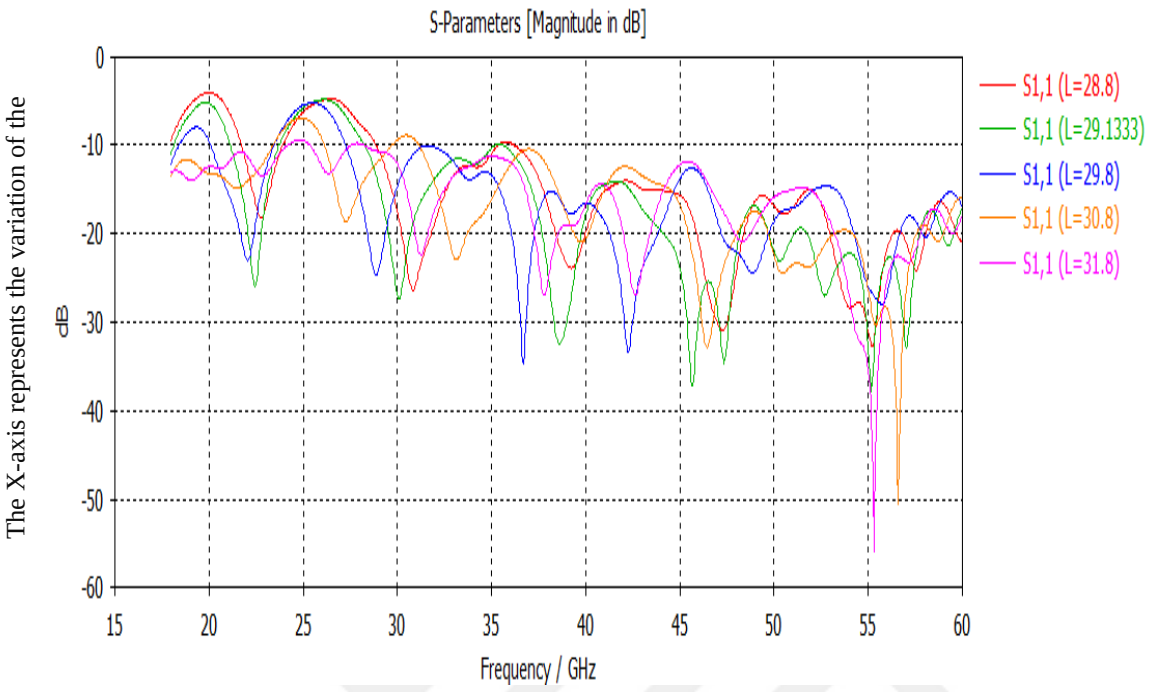

Figure 4. 2 S-parameter simulation for semi-rectangular patch antenna values of (L)

b. Effect of Substrate width (W)

The substrate width was simulated as the second parameter; this parameter has no significant impact on the bandwidth, so the small value that accomplished the bandwidth of ultra-wideband is (W = 17.2 mm). Fig (4.3) shows the parameter test to discover the most delicate esteem of this parameter, which gives optimum bandwidth from (28 GHz-60 GHz) with a reflection coefficient of $S11 \leq -10$ dB.

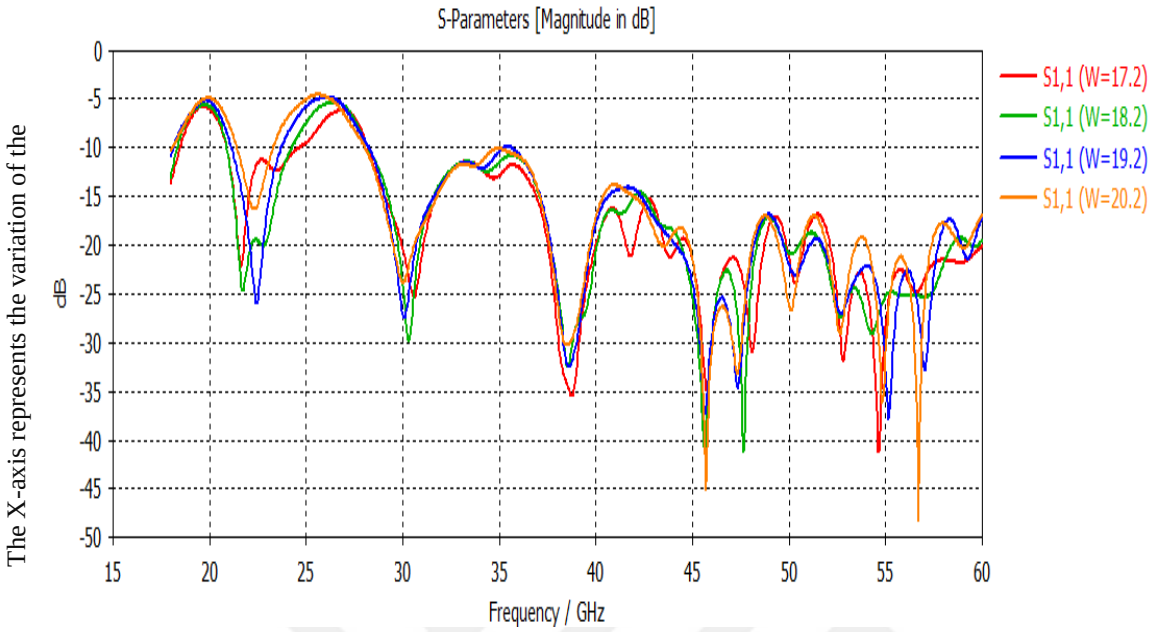

Figure 4. 3 S- simulation for a semi-rectangular patch antenna value of (W)

c. Effect of the minimum length of the antenna strip (L1)

The effect of the minimum length of the antenna strip (L1) was simulated as a third parameter; this parameter had no significant impact on the bandwidth, so the small value that accomplished the bandwidth of ultra-wideband is (L1 = 12.8 mm). Fig (4.4) shows the parameter test to discover the most delicate esteem of this parameter, which gives optimum bandwidth from (28 GHz-60 GHz) with a reflection coefficient of $S11 \leq -10$ dB.

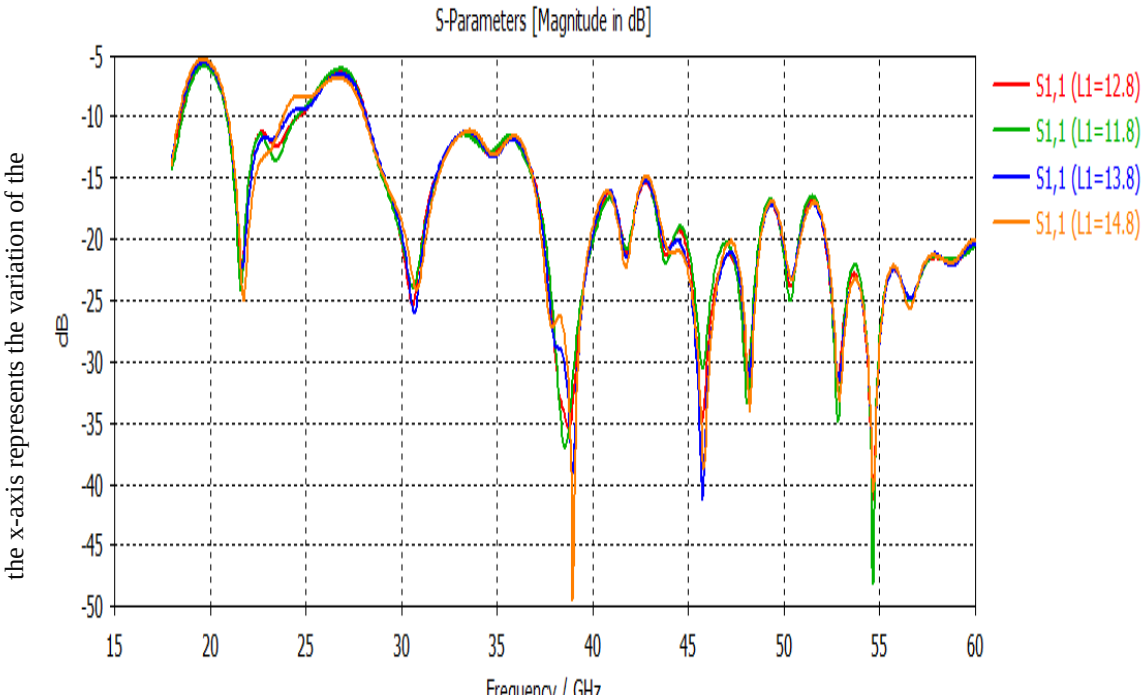

Figure 4. 4 Simulation of the S-parameter vs. frequency for the shortest antenna strip (L1)

c. Effect of the width of a rectangular hole in the antenna strip (M)

The fourth simulated parameter is the width of the semi-rectangular hole in the antenna strip (M), shown in Fig. (4-5). This Figure illustrates the simulation of the "S-parameter" for various values of the width of the rectangular hole in the antenna's ground. From the curve, it can be observed that (M = 2.7 mm) gives the best bandwidth from (28 to 60) GHz with a reflection coefficient of $S11 \leq -10$ dB.

The X-axis represents the variation of the

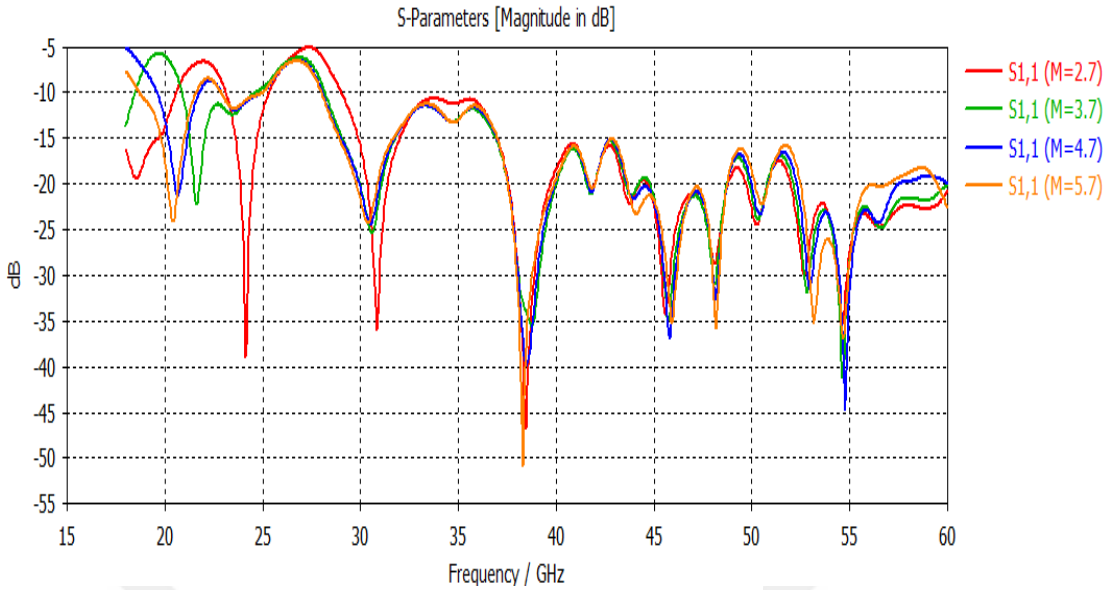

Y-axis represents the reflection confidence in dB

Figure 4. 5 Simulation of the S-parameter for the smallest rectangular hole in the antenna strip (M)

c. Effect of the width of a rectangular hole in the ground of the antenna (T)

The maximum width of the antenna strips is simulated as a third parameter. Fig. (4-6) illustrates the influence of changing the maximum width rectangular hole in the ground of the antenna (T) on the "S-parameter". From the curve, it is observed that the maximum width (T = 6.5 mm) gives preferable bandwidth from 28 GHz to 60 GHz with a reflection coefficient of $S11 \leq -10$ dB.

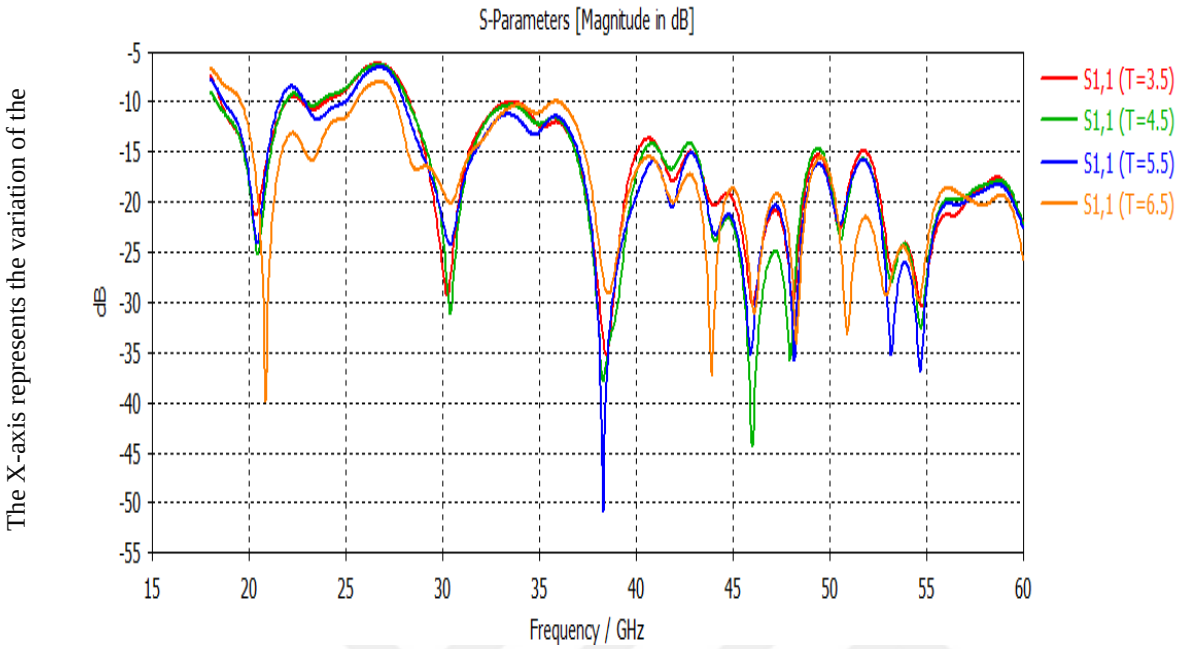

Figure 4. 6 S-parameter simulations for a rectangular hole with T values

d. Influence of Feeder Width Strip ($\mathbf{W_3}$)

The feeder width of the antenna strips was simulated as a fourth parameter. The influence of changing the feeder width of an antenna strip over the "S-parameter" appears in Fig. (4-7). By viewing the curve, it can be observed that the feeder width of the antenna strips (W3=3.2 mm) gives preferable bandwidth from (28 GHz) to (60 GHz) with a reflection coefficient of $S11 \leq -10$ dB.

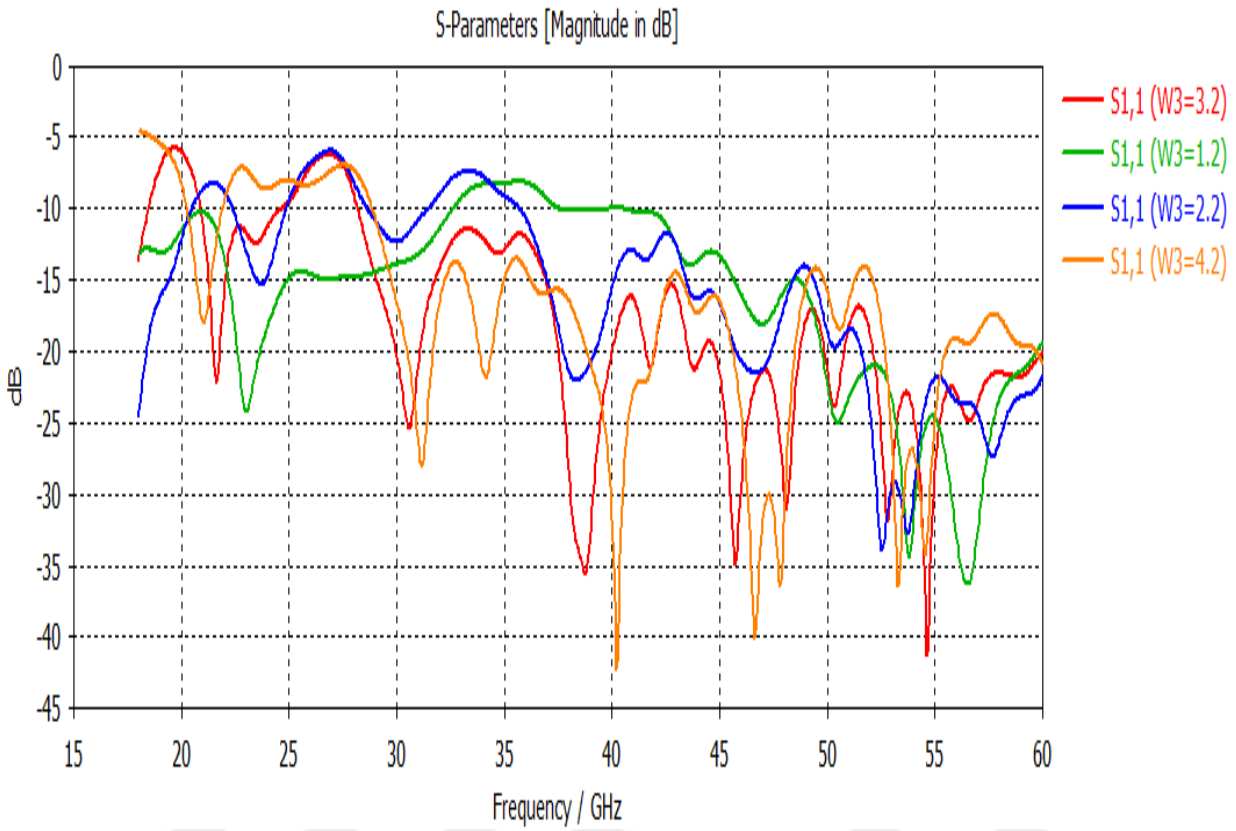

Figure 4. 7 S-parameter versus frequency simulation for a semi-rectangular patch antenna at various values of (W3)

4.2.3. Characteristics of Rectangular Patch Antenna

The characteristics of the suggested antenna with optimal parameter values. As shown in table 4.1:

Table 4. 1 Detailed Parameter for the Proposed Semi-Rectangular Patch Antenna

No.	Symbol	Definition	Size (mm)
1	L	Substrate length	29.133
2	W	Substrate width	17.2
3	L_1	The minimum length of the antenna strip	12.8
4	L_2	Length of the antenna ground	9.2
5	L_3	The minimum length of the border of the square hole in the ground of the antenna	1
6	L_4	The maximum length of the border of the square hole in the ground of the antenna	5.5
6	W_1	The maximum width of the antenna strips	5.2
7	T	The width of the square hole in the ground of the antenna	4.5
8	W_3	The width of the feeder strip	3.2
9	W_4	The width of the square hole in the patch of the antenna	3.7
10	L_c	The maximum length of the border of the antenna strip	19.2

. Fig. 4–8 showed the

a. Gain of the Antenna

suggested semi-rectangular patch of antenna's gain when it was simulated. From the curve, it is evident that the most extreme gain equal to 6 dB can be accomplished at (30.433 GHz), while the minor gain is equal to (0.8 dB) at (48 GHz), as shown in Fig (4-8. a). The x-axis represents the frequency variation in the GHz, while the y-axis represents the gain. The x-axis represents the frequency variation in the GHz, while the y-axis represents the gain.

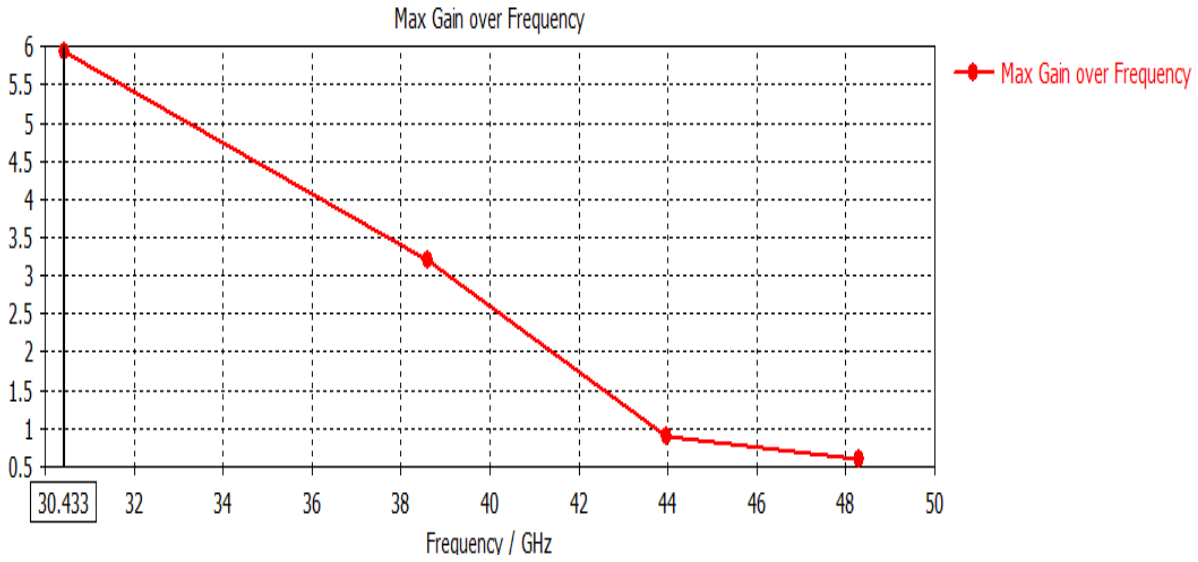

(a)

Fig (4-8. b). gain equal to (3.17 dB) can be accomplished onto (38.62 GHz).

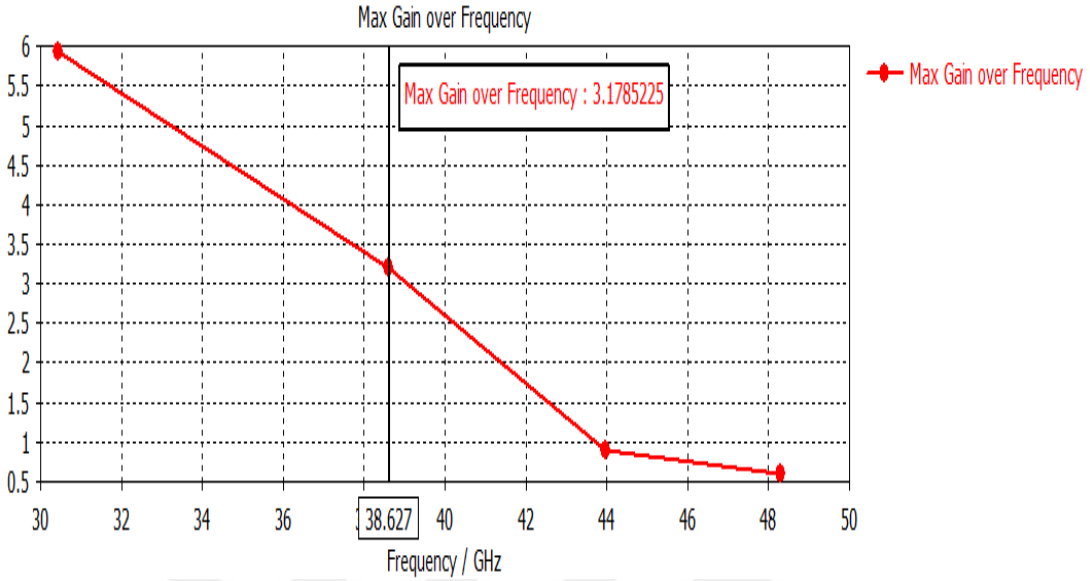

(b)

Fig(4-8.c) gain equal to (0.88 dB) can be accomplished onto (43.9 GHz).

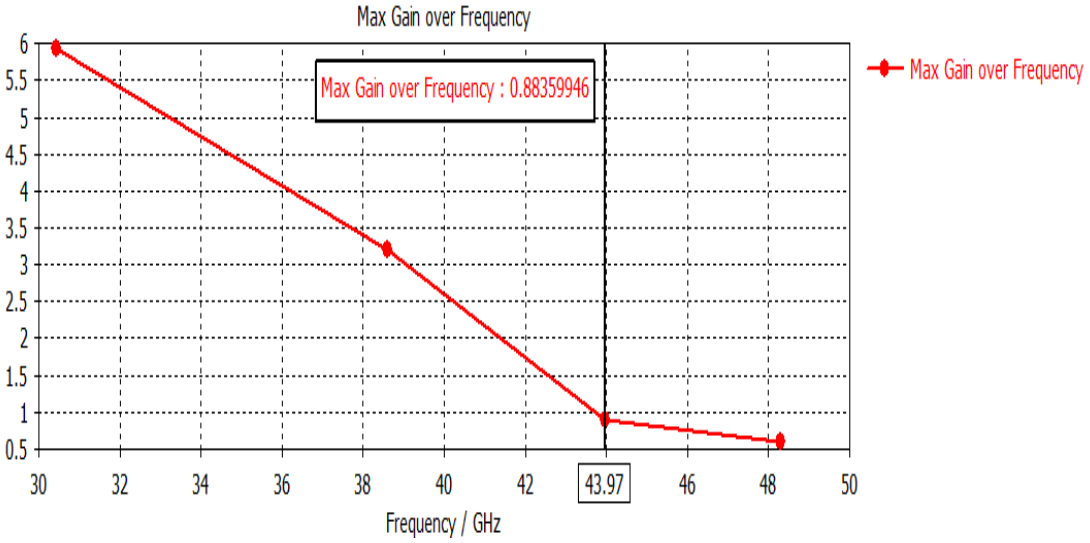

(c)

Fig (4-8. d) gain equal to (0.65 dB)

can be accomplished onto (48.2 GHz).

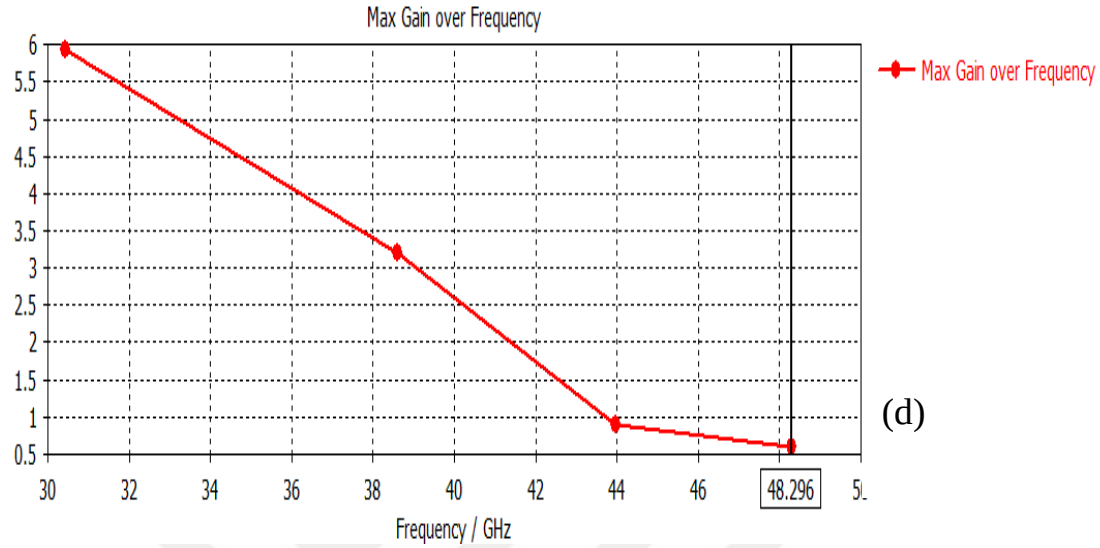

(d)

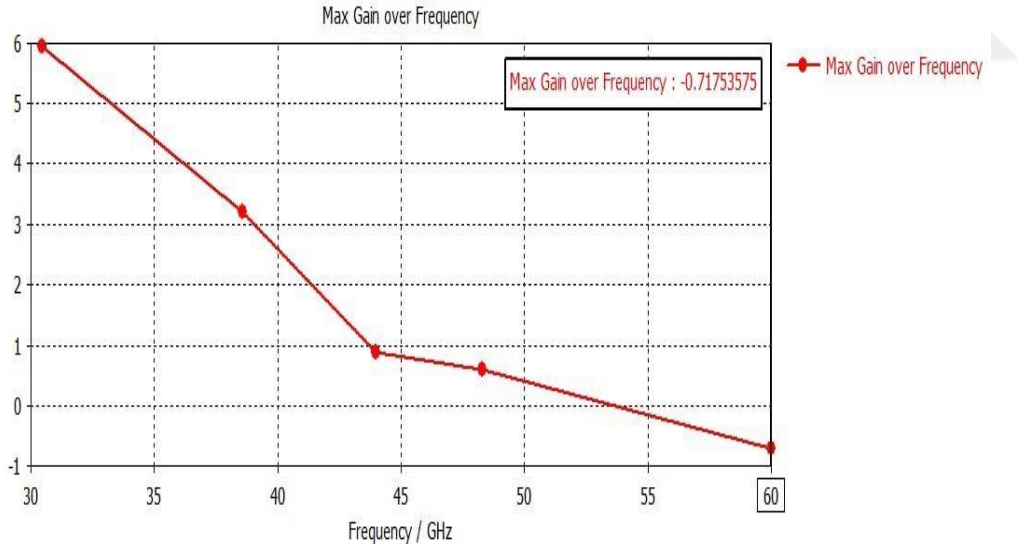

(C)

Figure 4. 8 Gain of a Semi-Rectangular Patch Antenna

S-parameter

The S-Parameter of the antenna against frequency is illustrated in Fig. (4-9). Results have shown that the proposed antenna achieved a bandwidth of 20–60 GHz. This band covers many applications such as WLAN, Wi-Fi, HIPERLAN-2, INSAT, Radio Astronomy Band, STM, and 5G mobile applications.

While the x-axis represents the frequency variation in the GHz

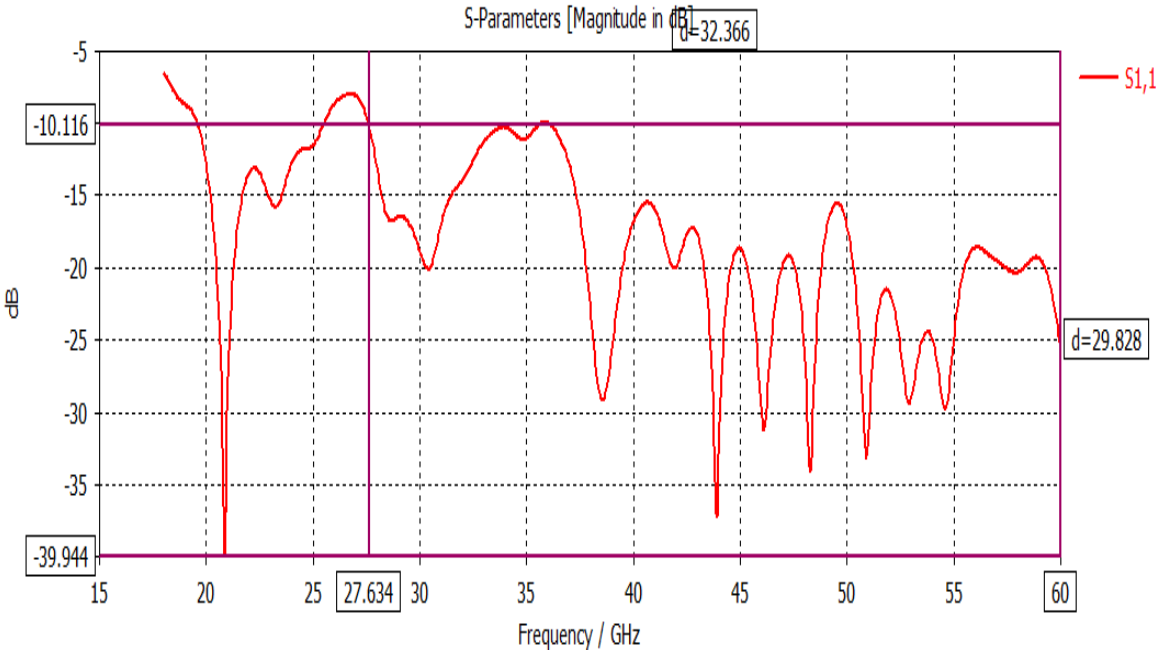

, the y-axis represents the reflection confidence in dB.

Figure 4. 9 S-P[illegible]ctangular al patch antenna.

b. “Voltage Standing Wave Ratio” (VSWR)

Fig. (4-10) explains VSWR against the frequency of a suggested antenna; from the curve, it is noticed that the value of VSWR is acceptable at the entire achieved band.

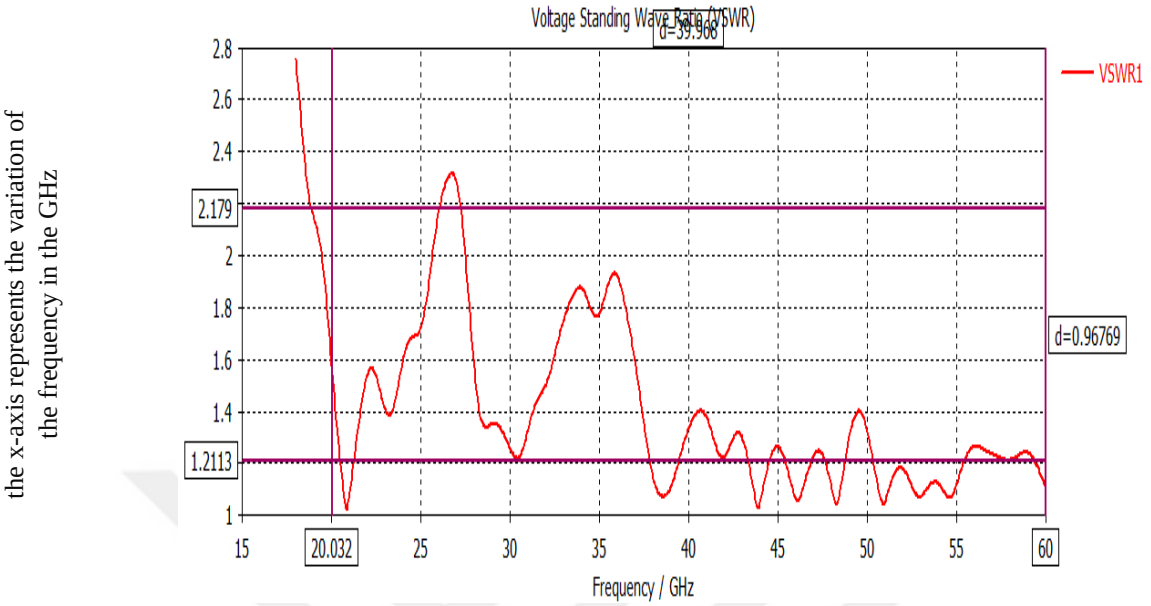

Figure 4. 10 VSWR simulation for a semi-rectangular al patch antenna

c. Input Impedance

Fig. (4-11) illustrates the impedance variation of the natural and imaginary parts with frequency.

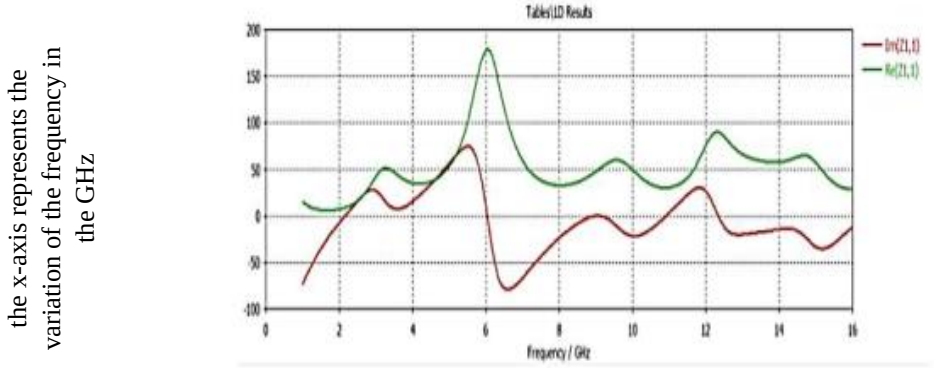

Figure 4. 11- Input impedance of proposed antenna

e. Current Distribution

The current distributions of the proposed antenna are shown in Fig. (4-12) at frequencies of (a) 30.4GHz, (b) 38.59, (c) 43.64, and (d) 48.29 GHz. Fig. (4-12, a) illustrates the value (101.438 A/m)

as a maximum current at the frequency of 30.4GHz, and Fig. (4-12, b) illustrates the value (108 A/m) as a maximum current at the frequency of 38.59 GHz.

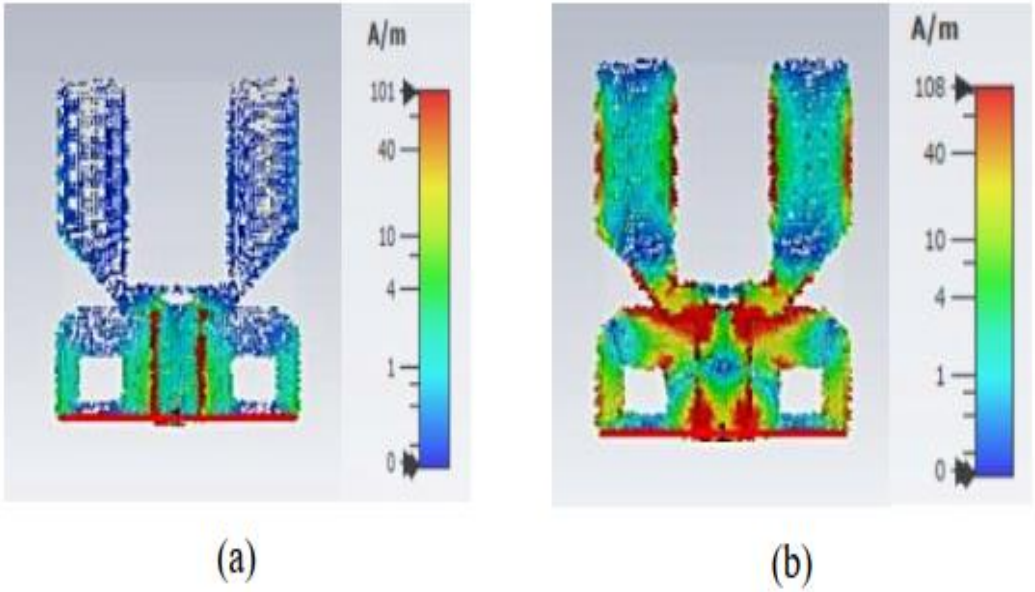

Figure 4. 12 Current frequency distributions at (a) 30.4 GHz and (b) 38.59 GHz.

f. 3D Radiation Pattern

For frequencies of 30.4 GHz and 38.59 GHz, the 3D radiation will be illustrated in Fig. (4-14). In this Figure, it is observed that the radiation pattern at 30.4 GHz has a maximum directivity of 2.86 dB, and at 9GHz, the maximum directivity is 6.3 dB. These designs have properties in general that achieve bandwidth, which is required for numerous applications.

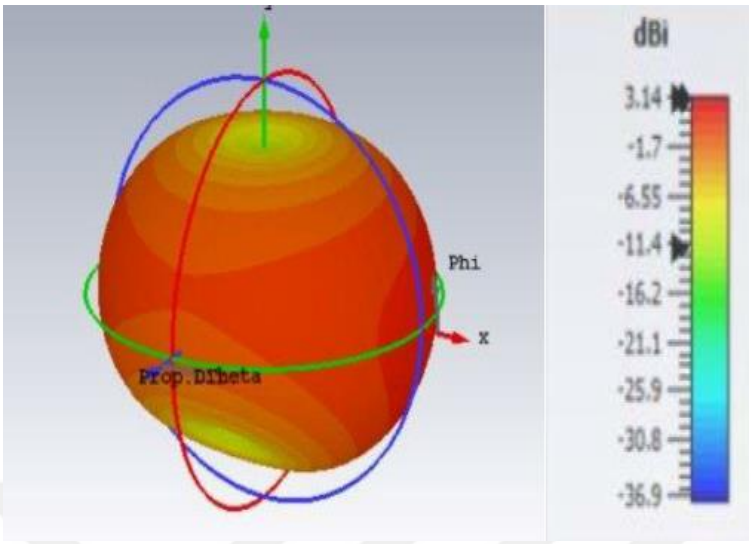

(a) F=30.4 GHz

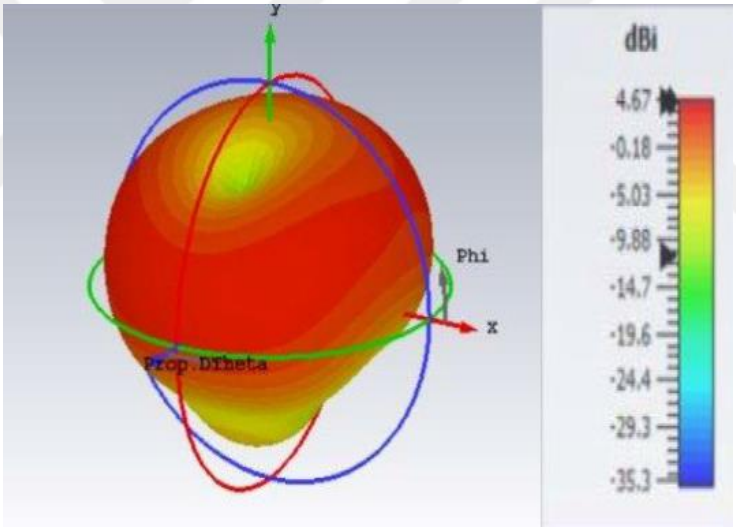

(b) F=38.59 GHz

Figure 4. 13
The radiation pattern for a semi-rectangular patch in three dimensions at various frequencies

4.3. Far filed Radiation Patterns

Radiation patterns simulation of the improved antenna in the "y-z" plane (Electric -plane) and "x-z" plane (Magnetic -plane) for four frequencies through the passband, which is equal to (30.4), (38.59), (43.64) and (48.29) GHz. Fig. (4-14, a) shows the Far field directivity at 30.4 GHz, for (Phi=90) Electric -the field has a primary lobe magnitude of 9.64 dB. in the direction 132 °and an angular width (3dB) is (17.5°).

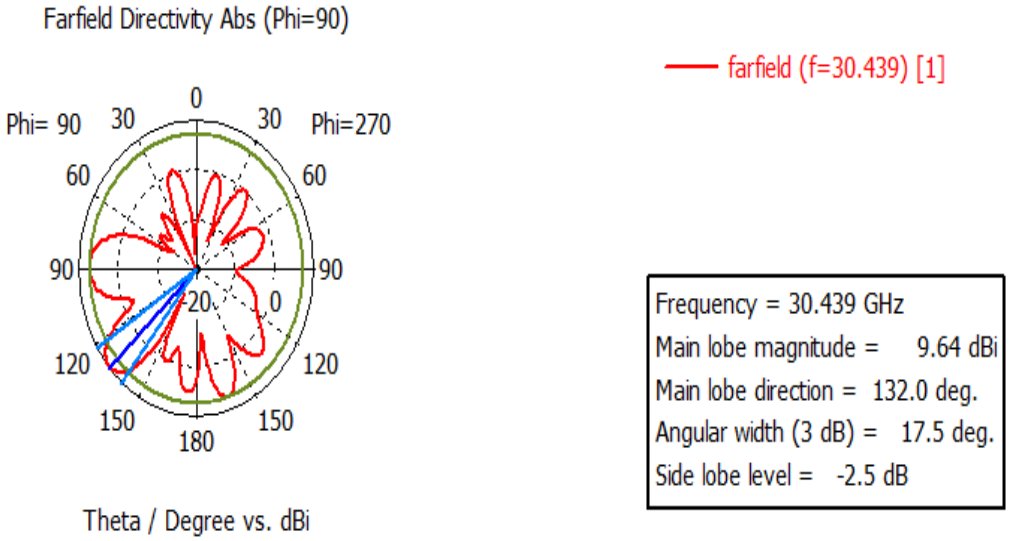

(a)

Fig. (4-14, b) shows the Far field directivity at 38.59 GHz for (Phi=90) E-filed has a primary lobe magnitude of 6.85 dB in the direction(91°) and an angular width (3dB) of (30.1◦).

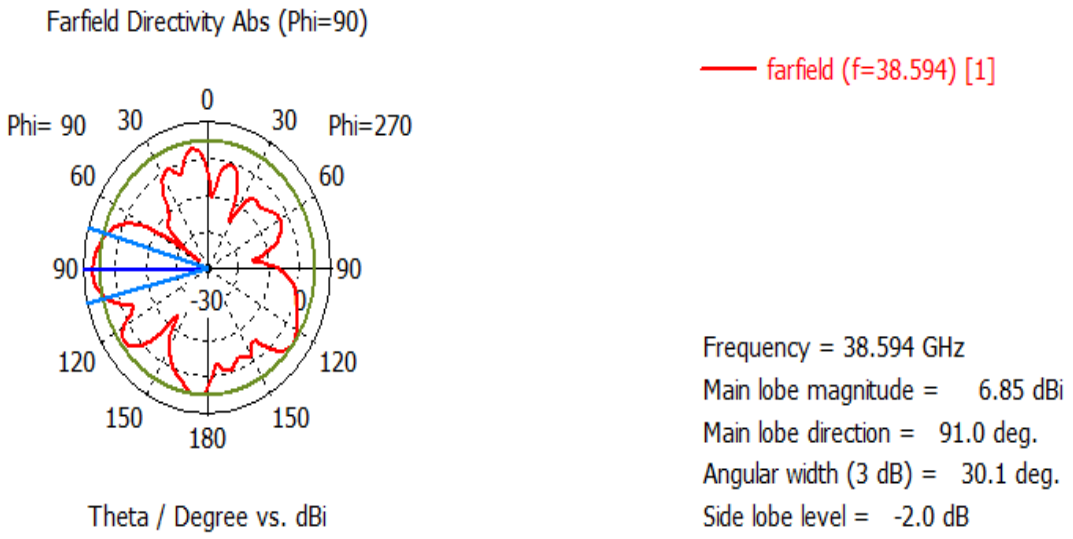

(b)

Fig. (4-14, c) the far field directivity at 43.964 GHz, for (Phi=90) E-filed, has a primary lobe magnitude of 6.56 dBi in the direction(35°) and an angular width (3dB) of (12.7◦).

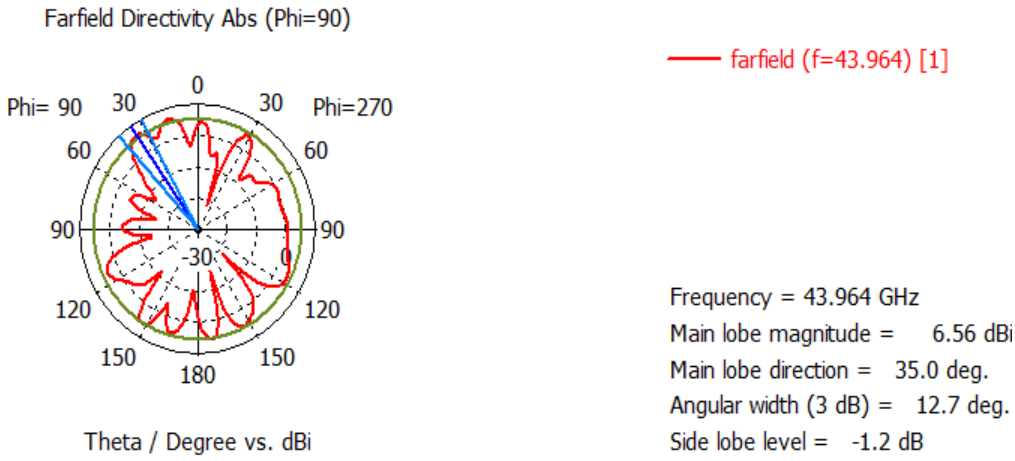

(c)

Fig. (4-14, d) shows the far field directivity at 48.29 GHz, for (Phi=90) E-filed has a main lobe a magnitude of 7.49 dBi in the direction(153.0◦) and an angular width (3dB) of (9.1◦).

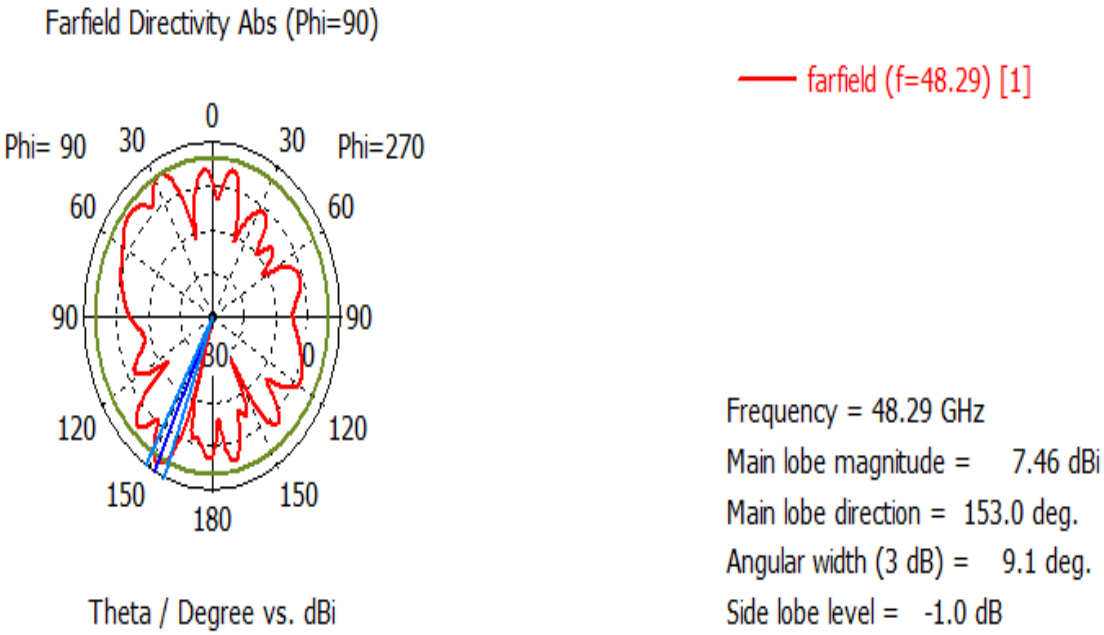

(d)

Figure 4. 14

Far filed patterns at (a) 30.4GHz, (b) 38.59 (c) 43.64

4.5 Manufacturing of the Proposed Semi-Rectangular Patch Antenna

In this part, the CST suit findings of the proposed antenna are compared with actual measurements to establish the design's validity. The manufacturing antenna results presenting in Figure.4.15, Semi-Rectangular Patch Antenna (The Front of The Antenna), and the Semi-Rectangular Patch Antenna (The Back of The Antenna.) are presented in figures 4.15 a and b, consequently. While the Figure 4.15.c representing the proposed antenna measure.

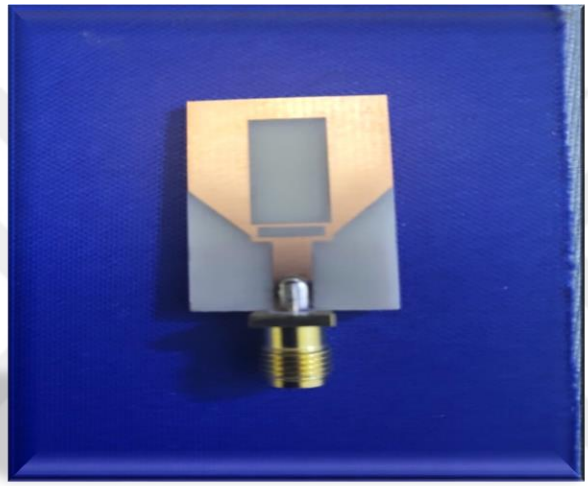

(a)

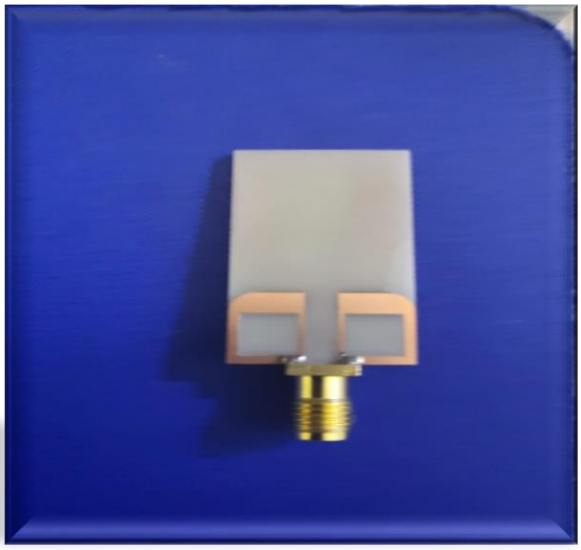

(b)

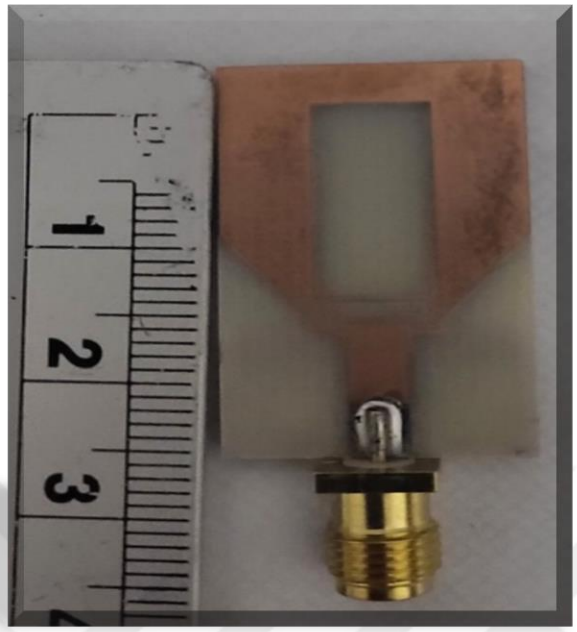

(c)

Figure 4. 15 Manufactured Semi-Rectangular Patch Antenna

CHAPTER FIVE

CONCLUSION AND RECOMMENDATIONS FOR FUTURE WORK

5.1. Conclusion

In this research, three antennas have been suggested and designed, which are helpful for many wireless application requirements. Excellent correspondence was obtained between measured and simulated information, covering the spectrum between 28 GHz and 60 GHz. The results of these three antennas affirm that it is reasonable for numerous UWB applications. The suggested designs give a sensible arrangement to the appropriateness of rectangular, circular, and elliptical patch antennas utilized in UWB applications. The following can be concluded from this study:

1. These two antennas are rivals in performance to some other large-size designs, which makes them more suitable for many critical wireless applications.

2. The shape of the ground in an antenna array has an essential effect on the antenna array characteristics such as bandwidth, current distribution, gain, impedance, and radiation pattern.

3. In the elliptical antenna, outstanding investigations were carried out to extract the time-domain behavior of the notch frequency antenna. Regardless of the notch's appearance in the frequency domain, the distortion of the transmitted and obtained signal is low, making it appropriate to use as a UWB antenna.

4. The results of the semi-rectangular patch antenna show that quite a large bandwidth from 27 GHz to 60 GHz has been produced for the suggested antenna that may be utilized in ultra-wideband communication systems.

5.2. Recommendations for Future Work

Recommendations for future work can be registered as follows:

1. How can minimizing the size of the designed antenna depend on fractal geometry?
2. Which shape of patch antenna can be designed to increase the obtained bandwidth?
3. How can the bandwidth and gain be improved by increasing the number of elements and modifying the ground plane?
4. Based on the acceptable results of these three antennas, how can they be improved to obtain higher bandwidth with a reduced size that could be a suitable choice for 4G and 5G mobile systems?

REFERENCES

Abbas, S. M., Ali, R. L., Nawaz, H., Kiyani, A., Saleem, I., & Khan, S. A. (2011). A compact microstrip patch antenna with a circular snipped slot for GSM, Wi-Fi, and WiMAX applications. Paper presented at the 2011 7th International Conference on Emerging Technologies.

Agarwal, A., Misra, G., & Agarwal, K. J. A. J. o. E., & Engineering, E. (2015). The 5th generation mobile wireless networks-key concepts, network architecture, and challenges. 3(2), 22-28.

Ahmed, W., Haggag, A., & Shaker, A. A Triple-U Triple-Domain Antenna Designed For Mobile Generations Supporting Up-To 5GH.

Aiello, R., & Batra, A. (2006). Ultra-wideband systems: technologies and applications: Elsevier.

Alhalabi, R. A. (2010). High efficiency planar and RFIC-based antennas for millimeter-wave communication systems: University of California, San Diego.

Alreshaid, A. T., Hammi, O., Sharawi, M. S., & Sarabandi, K. (2015a). A compact millimeter-wave slot antenna array for 5G standards. Paper presented at the 2015 IEEE 4th Asia-Pacific Conference on Antennas and Propagation (APCAP).

Alreshaid, A. T., Hammi, O., Sharawi, M. S., & Sarabandi, K. (2015b). A millimeter wave switched beam planar antenna array. Paper presented at the 2015 IEEE International Symposium on Antennas and Propagation & USNC/URSI National Radio Science Meeting.

Andrews, J. G., Buzzi, S., Choi, W., Hanly, S. V., Lozano, A., Soong, A. C., & Zhang, J. C. J. I. J. o. s. a. i. c. (2014). What will 5G be? , 32(6), 1065-1082.

Ashraf, M. A., Haraz, O. M., & Alshebeili, S. (2015). Compact size enhanced gain switched beam conformal antipodal tapered slot antenna system for 5G MIMO wireless communication. Paper presented at the 2015 IEEE 11th International Conference on Wireless and Mobile Computing, Networking and Communications (WiMob).

Balanis, C. (1997). Antenna analysis, theory, and design. In: Wiley.

Balanis, C. A. (2012). Advanced engineering electromagnetics: John Wiley & Sons.

Bankey, V., & Kumar, N. A. J. I. J. o. A. V. (2016). Design of a Yagi-Uda antenna with gain and bandwidth enhancement for Wi-Fi and Wi-Max applications. 2.

Basavarajappa, V., & Vinoy, K. J. P. I. E. R. B. (2010). An integrated wideband multifunctional antenna using a microstrip patch with two U-slots. 22, 221-235.

Bharti, P. K., Pandey, G. K., Singh, H. S., & Meshram, M. K. (2015). A compact multiband planar monopole antenna for slim mobile handset applications.

Chen, Z. N., See, T. S., Qing, X. J. I. T. o. a., & propagation. (2007). Small printed ultrawideband antenna with reduced ground plane effect. 55(2), 383-388.

Fang, D.-G. (2017). Antenna theory and microstrip antennas: CRC Press.

Fang, D. (2017). Microstrip patch antennas. In Antenna theory and microstrip antennas (pp. 85-110): CRC Press.

Fares, S. A., & Adachi, F. (2010). Mobile and Wireless Communications: Network Layer and Circuit Level Design: BoD–Books on Demand.

Federico, G., Caratelli, D., Theis, G., Smolders, A. J. I. J. o. A., & Propagation. (2021). A review of antenna array technologies for point-to-point and point-to-multipoint wireless communications at millimeter-wave frequencies. 2021.

Fung, C. J. W. P. I. (2011). Basic antenna theory and application. 18.

Gampala, G., & Reddy, C. (2016). Design of millimeter wave antenna arrays for 5G cellular applications using FEKO. Paper presented at the 2016 IEEE/ACES International Conference on Wireless Information Technology and Systems (ICWITS) and Applied Computational Electromagnetics (ACES).

Hong, W., Baek, K., Lee, Y., & Kim, Y. G. (2014). Design and analysis of a low-profile 28 GHz beam steering antenna solution for future 5G cellular applications. Paper presented at the 2014 IEEE MTT-S International Microwave Symposium (IMS2014).

Hong, W., Ko, S.-T., Lee, Y., & Baek, K.-H. (2015). Multi-polarized antenna array configuration for mmWave 5G mobile terminals. Paper presented at the 2015 International Workshop on Antenna Technology (iWAT).

Hsiao, F.-R. J. I. P. S. (2004). BROADBAND THIN INTERNAL PLANAR ANTENNA FOR MOBILE PHONE (YSTG). 12(4A2-4).

Hsu, C.-H., & Wu, P.-C. (2013). Microstrip-line-fed wide rectangular slot antenna for multiband operation. Paper presented at the 2013 IEEE International Wireless Symposium (IWS).

Jafarian, M., Kashani-Bozorg, S. F., Amadeh, A. A., & Atassi, Y. J. C. I. (2021). Hierarchical brain-coral-like structure (3D) vs rod-like structure (1D): Effect on electromagnetic wave loss features of SrFe12O19 and CoFe2O4. 47(21), 30448-30458.

Jayasinghe, J. W., Anguera, J., & Uduwawala, D. N. J. P. I. E. R. M. (2012). A simple design of multi-band microstrip patch antennas robust to fabrication tolerances for GSM, UMTS, LTE, and Bluetooth applications by using genetic algorithm optimization. 27, 255-269.

Jijo, B. T., Zeebaree, S., Zebari, R. R., Sadeeq, M., Sallow, A. B., Mohsin, S., & Ageed, Z. S. J. A. J. o. R. i. C. S. (2021). A comprehensive survey of 5G mm-wave technology design challenges. 8(1), 1-20.

Jing, X., Du, Z., Gong, K. J. I. A., & Letters, W. P. (2006). A compact multiband planar antenna for mobile handsets. 5, 343-345.

Kim, T., Bang, I., & Sung, D. K. (2014). Design criteria on a mmWave-based small cell with directional antennas. Paper presented at the 2014 IEEE 25th Annual International Symposium on Personal, Indoor, and Mobile Radio Communication (PIMRC).

Kuo, J.-S., Huang, C.-Y., & Jan, J.-Y. (2006). Planar monopole antenna for mobile phones on triple-frequency operation. Paper presented at the 2006 IEEE Antennas and Propagation Society International Symposium.

Kurup, H. B., Vijesh, K., Mohanan, P., Nampoori, V., & Bindu, G. (2014). A compact multi-band planar inverted-F antenna with reduced SAR for mobile terminals. Paper presented at the 2014 First International Conference on Computational Systems and Communications (ICCSC).

Li, Y., Li, W., Ye, Q., & Mittra, R. (2014). A survey of planar ultra-wideband antenna designs and their applications. Paper presented at the Forum for Electromagnetic Research Methods and Application Technologies (FERMAT).

Liu, Y., Sun, Q., Sharma, A., Sharma, A., & Dhiman, G. J. W. p. c. (2021). Line monitoring and identification based on roadmap towards edge computing. 1-24.

MacCartney, G. R., Zhang, J., Nie, S., & Rappaport, T. S. (2013). Path loss models for 5G millimeter wave propagation channels in urban microcells. Paper presented at the 2013 IEEE global communications conference (GLOBECOM).

Naser-Moghadasi, M., Sadeghzadeh, R., Asadpor, L., Virdee, B. J. I. a., & letters, w. p. (2013). A small dual-band CPW-fed monopole antenna for GSM and WLAN applications. 12, 508-511.

Nella, A., & Gandhi, A. S. (2017). A survey on microstrip antennas for portable wireless communication system applications. Paper presented at the 2017 International Conference on Advances in Computing, Communications and Informatics (ICACCI).

Nikmehr, S., & Moradi, K. (2010). Design and simulation of triple band GSM900/DCS1800/UMTS2100 MHz microstrip antenna for base station. Paper presented at the 2010 IEEE International Conference on Communication Systems.

Nor, N. M., Jamaluddin, M. H., Kamarudin, M. R., & Khalily, M. J. P. I. E. R. C. (2016). Rectangular dielectric resonator antenna array for 28 GHz applications. 63, 53-61.

Ojaroudiparchin, N., Shen, M., & Fr, G. (2015). Multi-layer 5G mobile phone antenna for multi-user MIMO communications. Paper presented at the 2015 23rd Telecommunications Forum Telfor (TELFOR).

Oppermann, I., Hämäläinen, M., & Iinatti, J. (2004). UWB: theory and applications: John Wiley & Sons.

Patil, S., & Rohokale, V. (2015). Multiband smart fractal antenna design for converged 5G wireless networks. Paper presented at the 2015 International Conference on Pervasive Computing (ICPC).

Pokorný, M., Horák, J., & Raida, Z. J. R. (2008). Planar tri-band antenna design. 17(1), 28-36.

Politano, C., Hirt, W., Rinaldi, N., Di Benedetto, M., Kaiser, T., & Molisch, A. J. U. C. S. A. C. O. (2006). Regulation and standardization. 5, 471-492.

Rahman, R., Morshed, K. M., Sabrin, S., & Rahman, M. (2015). Wideband planar monopole antenna for LTE, GSM, Bluetooth, WiMAX, DCS, PCS, and GPS mobile terminals. Paper presented at the 2015 2nd International Conference on Electrical Information and Communication Technologies (EICT).

Rathor, V. S., Saini, J. P. J. J. o. E. A., & Applications. (2014). A design of swastika-shaped wideband microstrip patch antenna for GSM/WLAN application. 2014.

Sabri, H., & Atlasbaf, Z. J. P. I. E. R. L. (2008). Two novel compact triple-band microstrip annular-ring slot antenna for PCS-1900 and WLAN applications. 5, 87-98.

Saleem, I., Nawaz, H., Shabbir, M. H., Abbas, S. M., & Ali, R. L. (2013). Ground plane tunable printed monopole antenna for wireless communications. Paper presented at the 2013 3rd IEEE International Conference on Computer, Control and Communication (IC4).

Senić, D., Živković, Z., Šimić, M., & Šarolić, A. (2014). Rectangular patch antenna: Design, wideband properties and loss tangent influence. Paper presented at the 2014 22nd International Conference on Software, Telecommunications and Computer Networks (SoftCOM).

Sharma, D., & Hashmi, M. S. (2014). A novel design of tri-band patch antenna for GSM/Wi-Fi/WiMAX applications. Paper presented at the 2014 IEEE International Microwave and RF Conference (IMaRC).

Singh, I., & Tripathi, V. J. I. J. C. T. A. (2011). Microstrip patch antenna and its applications: a survey. 2(5), 1595-1599.

Stutzman, W. L. J. I. A., & Magazine, P. (1998). Estimating directivity and gain of antennas. 40(4), 7-11.

Su, C.-M., Chien, S.-L., Tang, C.-L., & Wong, K.-L. (2005). A Novel Internal Mobile Phone Antenna for GSM/DCS Applications. Paper presented at the proceedings of the 8th biennial International Symposium on Communications (ISCOM 2005).

Tuovinen, T., Kumpuniemi, T., Yazdandoost, K. Y., Hämäläinen, M., & Iinatti, J. (2013). Effect of the antenna-human body distance on the antenna matching in UWB WBAN applications. Paper presented at the 2013 7th International Symposium on Medical Information and Communication Technology (ISMICT).

Vinci, G., & Weigel, R. (2010). Multiband planar Vivaldi antenna for mobile communication and industrial applications. Paper presented at the 2010 International Conference on Electromagnetics in Advanced Applications.

Wadekar, A. S., & Khobragade, S. V. (2015). Design of multiband monopole triangular fractal antenna for GSM, Bluetooth and Wi-Fi. Paper presented at the 2015 IEEE International Advance Computing Conference (IACC).

Wang, S., Lai, H. W., So, K. K., Ng, K. B., Xue, Q., Liao, G. J. I. A., & Letters, W. P. (2012). Wideband shorted patch antenna with a modified half U-slot. 11, 689-692.

Yu, A., Zhang, X. J. I. a., & letters, w. p. (2003). A novel method to improve the performance of microstrip antenna arrays using a dumbbell EBG structure. 2, 170-172.

Zhang, T., Li, R., & Tentzeris, M. M. (2011). Dual-frequency broadband antenna for mobile device applications. Paper presented at the 2011 IEEE International Symposium on Antennas and Propagation (APSURSI).

Zhao, H., Mayzus, R., Sun, S., Samimi, M., Schulz, J. K., Azar, Y., . . . Rappaport, T. S. (2013). 28 GHz millimeter wave cellular communication measurements for reflection and penetration loss in and around buildings in New York City. Paper presented at the 2013 IEEE international conference on communications (ICC).